Molecular Biology of the Cell
Vol. 17, 5211–5226, December 2006

C_2B Polylysine Motif of Synaptotagmin Facilitates a Ca^{2+}-independent Stage of Synaptic Vesicle Priming In Vivo

Carin A. Loewen,* Soo-Min Lee,† Yeon-Kyun Shin,† and Noreen E. Reist*

*Molecular, Cellular, and Integrative Neuroscience Program, Department of Biomedical Sciences, Colorado State University, Fort Collins, CO 80523; and †Department of Biochemistry, Biophysics, and Molecular Biology, Iowa State University, Ames, IA 50011

Submitted July 24, 2006; Revised September 6, 2006; Accepted September 7, 2006
Monitoring Editor: Jeffrey Brodsky

Synaptotagmin I, a synaptic vesicle protein required for efficient synaptic transmission, contains a highly conserved polylysine motif necessary for function. Using *Drosophila*, we examined in which step of the synaptic vesicle cycle this motif functions. Polylysine motif mutants exhibited an apparent decreased Ca^{2+} affinity of release, and, at low Ca^{2+}, an increased failure rate, increased facilitation, and increased augmentation, indicative of a decreased release probability. Disruption of Ca^{2+} binding, however, cannot account for all of the deficits in the mutants; rather, the decreased release probability is probably due to a disruption in the coupling of synaptotagmin to the release machinery. Mutants exhibited a major slowing of recovery from synaptic depression, which suggests that membrane trafficking before fusion is disrupted. The disrupted process is not endocytosis because the rate of FM 1-43 uptake was unchanged in the mutants, and the polylysine motif mutant synaptotagmin was able to rescue the synaptic vesicle depletion normally found in syt^{null} mutants. Thus, the polylysine motif functions after endocytosis and before fusion. Finally, mutation of the polylysine motif inhibits the Ca^{2+}-independent ability of synaptotagmin to accelerate SNARE (soluble *N*-ethylmaleimide-sensitive factor attachment protein receptor)-mediated fusion. Together, our results demonstrate that the polylysine motif is required for efficient Ca^{2+}-independent docking and/or priming of synaptic vesicles in vivo.

INTRODUCTION

Synaptotagmin I is a synaptic vesicle protein whose cytoplasmic region contains two C_2 domains, C_2A and C_2B (Perin *et al*., 1991; Brose *et al*., 1992). Although synaptotagmin is a Ca^{2+} sensor for synaptic vesicle exocytosis (Brose *et al*., 1992; Geppert *et al*., 1994), primarily via its C_2B Ca^{2+}-binding motif (Figure 1A, circles; Mackler *et al*., 2002; Nishiki and Augustine, 2004), it likely mediates other molecular interactions via additional functional motifs.

The C_2B domain of synaptotagmin contains a highly conserved polybasic region (Figure 1A, dashes; Rickman *et al*., 2004). Three lysines within this region (the polylysine motif; Figure 1A, asterisks) are required for full synaptotagmin function. In *Drosophila*, when these lysines are mutated to glutamines (syt^{KQ}) and the syt^{KQ} transgene is expressed in a syt^{null} background ($-/-;P[syt^{KQ}]$), evoked transmitter release is decreased compared with transgenic wild-type controls ($-/-;P[syt^{WT}]$) (Mackler and Reist, 2001). The function of the polylysine motif within the synaptic vesicle cycle remains controversial. Results from in vitro experiments suggest this motif may mediate three steps in the synaptic vesicle cycle: 1) endocytosis, 2) Ca^{2+}-triggered vesicle fusion, and 3) Ca^{2+}-independent docking and/or priming of synaptic vesicles.

Functional studies demonstrate that synaptotagmin I is required for synaptic vesicle endocytosis (von Poser *et al*., 2000; Jarousse and Kelly, 2001; Jarousse *et al*., 2003; Poskanzer *et al*., 2003; Llinás *et al*., 2004; Nicholson-Tomishima and Ryan, 2004), and in vitro studies suggest that the C_2B domain of synaptotagmin may mediate this role (von Poser *et al*., 2000; Jarousse and Kelly, 2001; Littleton *et al*., 2001; Jarousse *et al*., 2003; Llinás *et al*., 2004). Specifically, synaptic vesicle endocytosis may be mediated by the polylysine motif in the C_2B domain of synaptotagmin (Takei and Haucke, 2001; but see Poskanzer *et al*., 2006) via Ca^{2+}-independent interactions with the clathrin adaptor protein AP-2 (Zhang *et al*., 1994; Chapman *et al*., 1998; Haucke and De Camilli, 1999; Haucke *et al*., 2000; Littleton *et al*., 2001; Grass *et al*., 2004) and/or with phosphatidylinositol bisphosphate (PIP_2) (Bai *et al*., 2004). Both AP-2 and PIP_2 play a role in clathrin-mediated endocytosis (Cremona and De Camilli, 2001; Hurley and Wendland, 2002).

A second proposed function for the polylysine motif of synaptotagmin is regulation of Ca^{2+}-dependent processes (Chapman *et al*., 1998; Wu *et al*., 2003; Borden *et al*., 2005; Araç *et al*., 2006; Li *et al*., 2006). Polylysine motif mutations decrease the apparent Ca^{2+} affinity of synaptotagmin (Borden *et al*., 2005; Li *et al*., 2006). Furthermore, in vitro studies have implicated this motif in three Ca^{2+}-dependent processes: the ability of synaptotagmin to oligomerize (Chapman *et al*., 1998; Wu *et al*., 2003), the ability of synaptotagmin to simultaneously bind to two membranes (Araç *et al*., 2006), and the ability of synaptotagmin to bind to negatively charged phospholipids (Li *et al*., 2006). The Ca^{2+}-dependent oligomerization and phospholipid binding of

This article was published online ahead of print in *MBC in Press* (http://www.molbiolcell.org/cgi/doi/10.1091/mbc.E06–07–0622) on September 20, 2006.

Address correspondence to: Noreen E. Reist (reist@lamar.colostate.edu).

Abbreviations used: t-SNARE heterodimers, syntaxin/SNAP-25; v-SNARE, VAMP or synaptobrevin; SNARE complex, VAMP/syntaxin/SNAP-25; minis, miniature synaptic potentials.

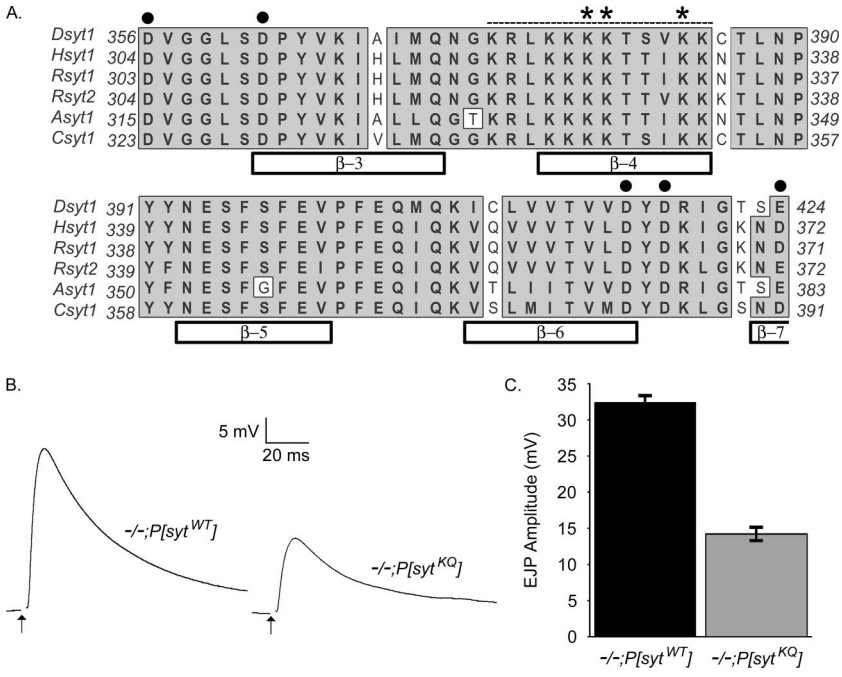

Figure 1. Synaptotagmin C_2B polylysine region is highly conserved throughout evolution and is required for efficient synaptic transmission. (A) ClustalW sequence alignment of 56 highly conserved amino acids from the C_2B domain of synaptotagmin. Bars indicate β-sheets within the C_2B domain. Circles mark the Ca^{2+}-binding motif. Dotted line denotes the polybasic region. Asterisks mark the polylysine motif. (B) Representative traces showing evoked release during 0.05-Hz stimulation in HL3 saline containing 1.5 mM Ca^{2+} in transgenic controls ($-/-;P[syt^{WT}]$) and polylysine motif mutants ($-/-;P[syt^{KQ}]$). Each trace is an average of 10–12 individual traces from a single muscle fiber. Stimulus artifact has been removed for clarity. (C) The mean EJP amplitude in saline containing 1.5 mM Ca^{2+} was 14.2 ± 0.82 mV (mean ± SEM; n = 34 fibers) for polylysine motif mutants and 32.4 ± 0.99 mV (mean ± SEM; n = 42 fibers) for transgenic wild-type controls ($p \ll 0.001$).

synaptotagmin have been proposed to regulate the opening, dilation, or stability of the fusion pore (Wang *et al*., 2001; Bai and Chapman, 2004; Li *et al*., 2006). The simultaneous binding of synaptotagmin to two membranes has been proposed to accelerate membrane fusion by bringing the synaptic vesicle and plasma membrane into proximity (Araç *et al*., 2006).

Finally, the polylysine motif may participate in a Ca^{2+}-independent interaction that either holds synaptic vesicles at release sites (docking) and/or subsequently increases their probability of release (priming). Priming likely consists of multiple maturation steps that transform vesicles from a docked but not releasable state, through multiple releasable states with differing release properties (Martin, 2003). In the absence of Ca^{2+}, the polylysine motif of synaptotagmin preferentially binds to PIP_2-containing membranes, potentially mediating vesicle docking via a *trans*-interaction between the synaptic vesicle and the plasma membrane (Bai *et al*., 2004; Li *et al*., 2006) where PIP_2 is predominantly located (Holz *et al*., 2000; Micheva *et al*., 2001). This interaction could also mediate Ca^{2+}-independent vesicle priming, because it increases the rate of synaptotagmin penetration into lipid membranes in vitro upon Ca^{2+} influx (Bai *et al*., 2004), which is postulated to be important for fusion (Bai *et al*., 2000, 2002; Wang *et al*., 2003; Rhee *et al*., 2005). Additionally, the polylysine motif of synaptotagmin binds to target membrane-soluble *N*-ethylmaleimide-sensitive factor attachment protein receptor (t-SNARE) heterodimers (syntaxin/synaptosome-associated protein 25 kDa [SNAP-25]) in the absence of Ca^{2+} (Rickman *et al*., 2004, 2006). This Ca^{2+}-independent interaction may prime vesicles by bringing the synaptic vesicle (v)-SNARE (vesicle-associated membrane protein [VAMP] or synaptobrevin) into proximity with the t-SNARE heterodimer, preparing the vesicle for Ca^{2+}-triggered fusion via formation or stabilization of the SNARE complex (VAMP/syntaxin/SNAP-25; Xu *et al*., 1999; Rickman *et al*., 2004, 2006; Bhalla *et al*., 2006). Indeed, inclusion of synaptotagmin in v-SNARE–containing vesicles directly accelerates SNARE-mediated membrane fusion in a Ca^{2+}-independent manner (Mahal *et al*., 2002).

Using *Drosophila* mutants, we show that the polylysine motif plays a role during synaptic vesicle recycling after endocytosis and before fusion. This role serves to increase the rate of recovery from synaptic depression and increase the efficacy of synaptic vesicle fusion in vivo. Using a fluorescent lipid mixing assay, we show that the polylysine motif mediates the Ca^{2+}-independent ability of synaptotagmin to accelerate SNARE-mediated fusion. We discuss these results in the context of a single deficit hypothesis where the polylysine motif plays an important role in Ca^{2+}-independent docking/priming of synaptic vesicles.

MATERIALS AND METHODS

Fly Stocks

The polylysine motif (Figure 1A, asterisks) of *Drosophila* synaptotagmin was mutated ($K_{379,380,384}Q$), and the mutant synaptotagmin was expressed from a transgene in a *synaptotagmin* null (syt^{AD4}) line. The experimental flies ($-/-;P[syt^{KQ}]$) had the genotype *yw; syt*^{AD4} *P*[*elav-Gal4*]/*syt*^{AD4};*P*[*UAS syt*^{K379,380,384Q}]/+ and were generated as described previously (Mackler and Reist, 2001). The control flies ($-/-;P[syt^{WT}]$) expressed wild-type synaptotagmin I from a transgene (Mackler and Reist, 2001) and had the genotype *yw; syt*^{AD4} *P*[*elav-Gal4*]/*syt*^{AD4};*P*[*UAS syt*^{WT}]/+. Two independent transgenic wild-type *synaptotagmin* lines and two independent transgenic C_2B polylysine motif lines were generated. Because both lines of a given genotype had similar levels of evoked release (control lines [our unpublished data]; mutant lines, Mackler and Reist, 2001), one control line (2C) and one mutant line (#59) were used in subsequent experiments.

Solutions

Standard saline for these experiments is composed of 5 mM KCl, 2 mM $CaCl_2$, 130 mM NaCl, 2 mM $MgCl_2$, 36 mM sucrose, and 5 mM HEPES, pH 7.3 (Jan and Jan, 1976). In Ca^{2+}-free saline, the $CaCl_2$ was replaced by additional $MgCl_2$. Stimulating saline contained 90 mM KCl, 5 mM $CaCl_2$, 45 mM NaCl, 2 mM $MgCl_2$, 36 mM sucrose, and 5 mM HEPES, pH 7.3. HL3 saline contained 5 mM KCl, 70 mM NaCl, 20 mM $MgCl_2$, 10 mM $NaHCO_3$, 5 mM HEPES, 115 mM sucrose, 5 mM trehalose, and 1.5 mM $CaCl_2$ (Stewart *et al*., 1994). For the Ca^{2+} dependence curves, the $CaCl_2$ concentration in the HL3 saline varied (0.3, 0.5, 0.6, 0.8, 1.0, 1.5, 2.5, 3.5, 5.0, or 6.0 mM), whereas the $MgCl_2$ concentration was held constant at 20 mM. Hyperosmotic saline consisted of HL3 saline containing 0.8 mM Ca^{2+} and 0.5 M sucrose.

Dye Uptake Assay

Synaptic boutons in *Drosophila* third instars were labeled with the activity-dependent, fluorescent dye FM 1-43 (Invitrogen, Carlsbad, CA). Larvae were

dissected in Ca^{2+}-free saline, stimulated for 6 min with stimulating saline, and then the stimulating saline was replaced with standard saline containing 3 μM tetrodotoxin (TTX) for a variable length of time ($\Delta t = 0$, 30, 60, or 180 s). TTX was added to block spontaneous activity coming from the attached CNS. After Δt, the preparation was incubated in standard saline + 3 μM TTX + 4 μm FM 1-43 dye for 6 min to load endocytosing vesicles, and then it was washed for 15 min with three changes of Ca^{2+}-free saline to remove excess extracellular dye.

Fluorescence Microscopy and Image Processing

FM 1-43–labeled preparations were viewed using a 40×/0.80 numerical aperture water immersion objective lens (Leica, Bannockburn, IL) on a DMRA light microscope (Leica, Nussloch, Germany) equipped with epifluorescence optics (51019 EGFP/DsRed filter; Chroma Technology, Brattleboro, VT) and fitted with a microstepping servomotor in the *z*-axis. Images were captured with a Hamamatsu charge-coupled device camera (C4742–95). A through focal series by using 0.4-μm steps was taken of each labeled neuromuscular junction. All imaging was accomplished within 2 min of first exposure to light. Images were acquired, stored, and processed using Open Lab 2.2.0 software (Improvision, Boston, MA) on a Mac G-4 platform.

The average fluorescence intensity of 12–15 brightly stained boutons with diameters $\geq$2 μm were measured at each neuromuscular junction. Only boutons on muscle fibers 6 and 7 from segment 3 or 4 were used. Only one neuromuscular junction per preparation was imaged. Nine neuromuscular junctions (from 9 larvae) were analyzed for each genotype. Each bouton was imaged in its optimal focal plane. Images were imported into the public domain Object Image program (http://simon.bio.uva.nl/object-image.html). Background fluorescence was measured over nearby muscle nuclei and was subtracted from the fluorescence intensity of each bouton. Statistical comparisons between genotypes were tested with a mixed model analysis of variance (ANOVA) by using SAS software 6.12 (SAS Institute, Cary, NC).

Electrophysiology

Electrophysiology experiments were performed at room temperature in HL3 saline (Stewart *et al*., 1994) containing variable levels of Ca^{2+} (see above). Recordings were from muscle fiber 6 from abdominal segments 3 and 4 of third instar fillet preparations. Fibers were impaled with 15- to 45-MΩ electrodes filled with a solution of 3 parts 2 M potassium citrate to 1 part 3 M potassium chloride or a 4 M potassium acetate solution. Segmental nerves were stimulated with a 5- to 10-μm diameter glass micropipette filled with HL3 to evoke excitatory junctional potentials. Nerves were stimulated with 1-ms pulses at the indicated frequency, and voltage traces were collected using an AxoClamp 2B (Molecular Devices, Sunnyvale, CA) and digitized using a MacLab4s A/D converter (Chart or Scope software; ADInstruments, Colorado Springs, CO). The resting membrane potential of each muscle fiber was normally between -65 and -45 mV but was maintained at about -55 mV by passing a bias current. KaleidaGraph software (Synergy Software, Reading, PA) was used to fit linear regression lines to the data in Figure 3B and the Hill equation $[(\text{Max} \times [Ca^{2+}]^n)/(EC_{50}{}^n + [Ca^{2+}]^n)]$ to the data in Figure 3, A and C.

Hyperosmotic saline was pressure injected with a PLI-100 PICO-INJECTOR (Medical Systems, Greenvale, NY) onto the neuromuscular junction for 10 s with an injection pressure of 1.0 psi by using a glass micropipette with a tip diameter $<$1 μm. The recording electrode impaled the muscle at the extreme posterior end of the muscle, outside the area of hyperosmotic saline application, to reduce nonspecific leak current (Aravamudan *et al*., 1999). Voltage traces were collected as described above. In a blind analysis, the number of quantal events within 1-s intervals was binned during the 10-s hyperosmotic puff as well as during the 10 s before and after the puff.

Immunohistochemistry

Experimental and control third instars were dissected in the same dish in cold Ca^{2+}-free HL3 saline; fixed in 4% paraformaldehyde in phosphate-buffered saline (PBS); rinsed in PBS containing 0.1% Triton X-100 and 0.02% azide (PBST); and incubated overnight at 4°C in monoclonal antibody (mAb) nc82 (Developmental Studies Hybridoma Bank, University of Iowa, Iowa City, IA), diluted 1:100 in PBST containing 5% normal goat serum (PBST-NGS) and anti-GluRIII antibody (Marrus *et al*., 2004), diluted 1:200 in PBST-NGS. The preparations were washed in PBST, incubated for 1 h in Alexa Fluor 488 goat anti-mouse IgG (Invitrogen), diluted 1:500 in PBST-NGS and Texas Red goat anti-rabbit IgG (Jackson ImmunoResearch Laboratories, West Grove, PA), diluted 1:200 in PBST-NGS. Preparations were washed in PBST and mounted in Citifluor AF-1 (Ted Pella, Redding, CA).

Neuromuscular junctions from abdominal segments 3 or 4 were imaged on a Zeiss LSM 510Meta confocal microscope (Carl Zeiss Microimaging, Thornwood, NY) equipped with argon and HeNe1 lasers. Emissions were collected using a band pass 505–530 emission filter (for Alexa Fluor 488) or a long pass 585 emission filter (for Texas Red). Images were collected at 40 and 63× (pinhole set for 1 Airy unit for each), and confocal settings were adjusted to optimize the intensity range of the signal. For all images used for quantitative analysis, the settings were held constant between control and experimental preparations. Eight-bit images were acquired and *z*-stacks were converted to projections using Zeiss LM510 software.

For analysis, a region of interest (ROI) of constant area was drawn around each synaptic arborization as well as around a nearby area that contained only background staining. The histogram function of the software was used to determine the absolute number of pixels at every intensity (0–255) in these ROIs. To determine the intensity range of the signal (i.e., the range where the number of pixels in the signal was consistently greater than the number of pixels in the background), the number of pixels in the background ROI was subtracted from the number in the ROI containing the stained arborization for each intensity level. Once the intensity range of the signal was determined, the area of the signal was calculated by summing the number of pixels in the signal range. For Figure 2, the gamma setting of a Codonics NP-1600 Photographic Network Printer was adjusted to match the image appearance on the screen.

Electron Microscopy

Third instars were dissected in cold Ca^{2+}-free HL3 saline and then embedded, sectioned, and stained as described previously (Reist *et al*., 1998). Electron micrographs of neuromuscular junctions on muscle fiber number 6 and 7 from abdominal segments 3 or 4 were taken at 15,000× magnification on a JEOL JEM 2000 EX-II transmission electron microscope operated at 100 kV. Images were scanned using an Agfa DuoScan T2500 and adjusted for contrast using Adobe Photoshop software (Adobe Systems, Mountain View, CA).

Plasmid Construction and Site-directed Mutation for Fusion Proteins

Syntaxin 1A (amino acids 4-288), SNAP-25 (amino acids 1-206), and VAMP2 (amino acids 1-116) from rat were all inserted into pGEX-KG (between EcoRI and HindIII sites) as glutathione *S*-transferase (GST) fusion proteins. Four native cysteines in SNAP-25, one in VAMP2 and three in syntaxin 1A, were replaced with alanines. The plasmid for rat *synaptotagmin I* with a truncated luminal domain (amino acids 57-421) was inserted into pET-28 (b) (between NcoI and XhoI) as a C-terminal His_6-tagged protein. Among six native cysteines of synaptotagmin I, five cysteines located in the transmembrane domain were changed to alanines. The triple mutant ($K_{326,327,331}Q$) was made using a QuikChange site-directed mutagenesis kit (Stratagene, La Jolla, CA). The DNA sequences were confirmed by DNA sequencing (Iowa State University DNA Sequencing Facility, Ames, IA).

Protein Expression and Purification

The details of protein expression and purification were described previously (Lu *et al*., 2005; Xu *et al*., 2005). Briefly, GST-tagged proteins were expressed in *Escherichia coli* Rosetta (DE3) pLysS (Novagen, Madison, WI). GST fusion proteins were purified by affinity chromatography using glutathione-agarose beads (Sigma-Aldrich, St. Louis, MO). To purify proteins, the cell pellet was resuspended in 10 ml of PBST buffer [phosphate-buffered saline, pH 7.4, with 0.5% (vol/vol) Triton X-100] with the final concentrations of 1 mM 4-(2-aminoethyl)benzenesulfonyl fluoride (AEBSF), 1 mM EDTA, and 5 mM dithiothreitol (DTT). *n*-Lauroyl sarcosine (0.5%) was added to the solution. Cells were broken by sonication on the ice bath and centrifuged at 13,000 × *g* for 20 min at 4°C. The supernatant was mixed with 5 ml of glutathione-agrose beads (50%) in PBST buffer and incubated in the cold room for 2 h. During incubation for binding, 20 μg/ml DNase I and 4 μg/ml RNase were added. The beads were then washed with PBST buffer 10 times. The GST-tagged proteins were cleaved by bovine thrombin (Calbiochem, San Diego, CA) in PBS buffer containing 1% *n*-octyl-D-glucopyranoside (OG).

The His-tagged synaptotagmin I was expressed in *E. coli* condon plus (BL21) pLysS (Stratagene) and induced by 0.3 mM isopropyl-D-galactopyranoside. The cell pellet was sonicated and centrifuged in 10 ml of lysis buffer (25 mM HEPES, 400 mM KCl, 10 mM imidazole, 2 mM EDTA, 2 mM AEBSF, 2 mM DTT, 0.5% Triton X-100, and 0.5% *n*-lauryl sarcosine, pH 7.4). The supernatant was mixed with 2 ml of nickel-nitrilotriacetic acid (Ni-NTA) agarose beads (QIAGEN, Valencia, CA). DNase I and RNase were added to the supernatant and the Ni-NTA beads mixture. After binding for 2 h at 4°C, Ni-NTA beads were washed with wash buffer six times. Synaptotagmin I was eluted in elution buffer (25 mM HEPES, 400 mM KCl, 400 mM imidazole, and 1% OG, pH 8.0). Purified proteins were examined with 15% SDS–PAGE, and the purity was at least 90% for all proteins.

Membrane Reconstitution

The procedure was described previously (Lu *et al*., 2005, 2006). Briefly, syntaxin 1A was incubated with SNAP-25 for 1 h at room temperature to allow the formation of t-SNARE complex. The liposomes containing 1-palmitoyl-2-dioleoyl-sn-glycero-3-phosphatidylcholine (POPC) and 1,2-dioleoyl-*sn*-glycero-3-phosphatidylserine (DOPS) (molar ratio 85:15; 50 mM) were reconstituted with the preformed t-SNARE complex in a lipid/protein ratio of 200:1. The fluorescent liposomes containing POPC, DOPS, 1,2-dioleoyl-*sn*-glycero-3-phosphoserine-*N*-(7-nitro-2–1,3-benzoxadiazol-4-yl) (NBD-PS), and 1,2-dioleoyl-*sn*-glycero-3-phosphoethanolamine-N-(lissamine rhodamine B sulfonyl) (rhodamine-PE) (molar ratio of 83:15:1:1; 10 mM) were reconstituted with

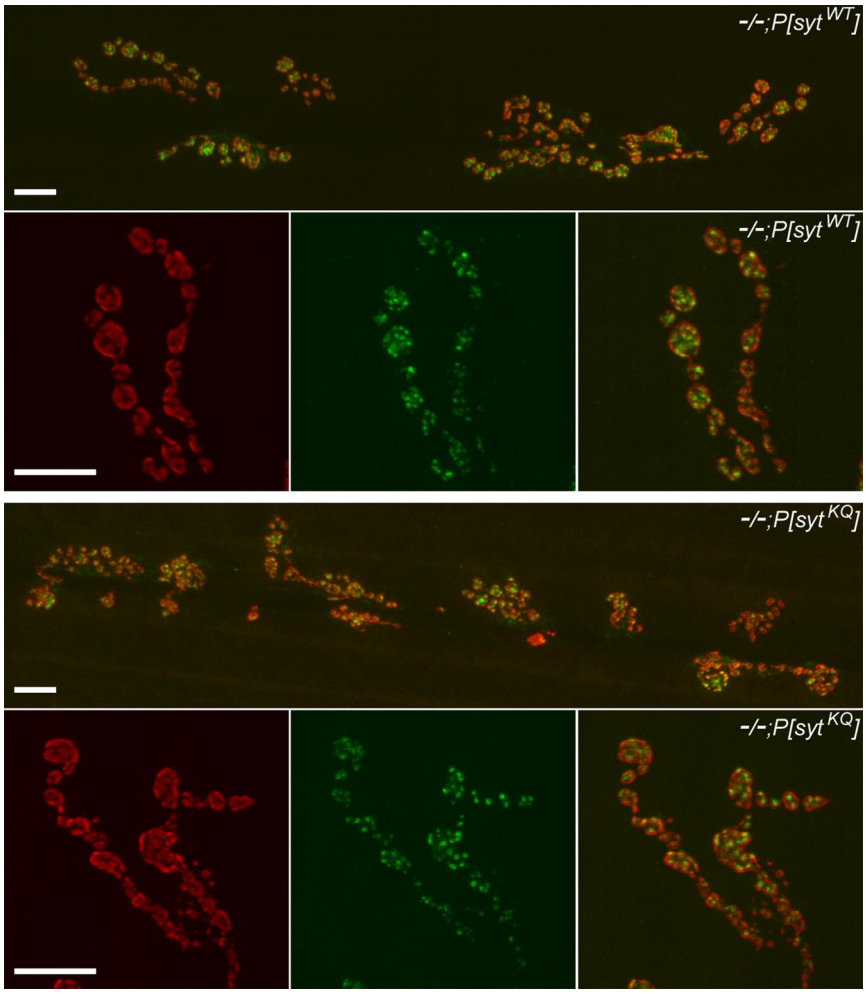

Figure 2. GluRIII and nc82 antibody staining was unchanged in polylysine motif mutants. Representative 40 and 63× images of neuromuscular junctions from transgenic controls ($-/-;P[syt^{WT}]$, top) and polylysine motif mutants ($-/-;P[syt^{KQ}]$, bottom). Junctions were stained with an anti-GluRIII antibody (red) to show postsynaptic receptors, and they were stained with mAb nc82 (green) to show active zones. Bar, 10 μm.

VAMP2 in 200:1 lipid/protein ratio. Synaptotagmin I was reconstituted with VAMP2 (molar ratio 1:1). To remove OG, the samples were diluted two times with dialysis buffer (25 mM HEPES and 100 mM KCl, pH 7.4) and then dialyzed against 2 liters of dialysis buffer at 4°C overnight. After dialysis, the solution was centrifuged at 10,000 × *g* to remove protein and lipid aggregates. The reconstitution efficiencies were determined using SDS-PAGE and were at least 70%.

Total Fluorescence Lipid Mixing Assay

To measure the lipid mixing, v-SNARE liposomes with or without synaptotagmin I were mixed with t-SNARE liposomes in the ratio of 3:7. The final solution for each reaction contained ~1 mM lipids in HEPES buffer (25 mM HEPES and 100 mM KCl, pH 7.4, and 5% glycerol) with the total volume of 100 μl. Fluorescence intensity was monitored with the excitation and emission wavelengths of 465 and 530 nm, respectively. The fluorescence signal was recorded using a Varian Cary Eclipse model fluorescence spectrophotometer with a quartz cell of 100 μl with a 2-mm path length. After 4000 s, 0.25% *n*-dodecylmaltoside was added to obtain the maximum fluorescence intensity. All of the lipid mixing experiments were carried out at 35°C.

RESULTS

Synaptic Transmission Is Disrupted in Synaptotagmin Polylysine Motif Mutants

The C_2B polylysine motif of synaptotagmin I is required for efficient synaptic transmission (Figures 1, B and C, and 3; Mackler and Reist, 2001; Borden *et al*., 2005; Li *et al*., 2006). We examined excitatory junctional potentials (EJPs) in *Drosophila synaptotagmin* null third instars that expressed either a wild-type *synaptotagmin* transgene ($-/-;P[syt^{WT}]$) or a C_2B-polylysine motif mutant transgene ($-/-;P[syt^{KQ}]$). Figure 1B shows representative traces recorded in saline containing 1.5 mM Ca^{2+}. Because both the polylysine motif transgene and the control transgene exhibit similar levels of synaptotagmin expression (Mackler and Reist, 2001), the only difference between these lines is the mutation in the C_2B polylysine motif of synaptotagmin. Figure 1C illustrates that the average EJP amplitude at third instar neuromuscular junctions in saline containing 1.5 mM Ca^{2+} was 14.2 ± 0.82 mV for polylysine motif mutants ($-/-;P[syt^{KQ}]$; n = 34 fibers) and 32.4 ± 0.99 mV for transgenic wild-type controls ($-/-;P[syt^{WT}]$; n = 42 fibers). Thus, similar to what has been reported previously for this synapse (Mackler and Reist, 2001), evoked transmitter release in 1.5 mM Ca^{2+} was decreased in polylysine motif mutants to ~45% of transgenic controls.

The Postsynaptic Responsiveness Is Not Changed in Synaptotagmin Polylysine Motif Mutants

To verify that the decrease in the evoked response was not due to a developmental disruption that resulted in a reduced number of postsynaptic glutamate receptors or presynaptic active zones, we examined GluRIII (Marrus *et al*., 2004) and nc82 (an active zone marker; Wucherpfennig *et al*., 2003; Qin *et al*., 2005) staining in polylysine motif mutants and controls (Figure 2). The area of GluRIII staining [polylysine motif mutants, 49,500 ± 6600; transgenic controls,

47,000 ± 5500 pixels at 40× magnification (mean ± SEM)] was not significantly different in polylysine motif mutants compared with transgenic controls ($p > 0.78$, Student's *t* test; n = 6 junctions for each genotype). In addition, the amplitude of spontaneous fusion events is unchanged in the mutants (Mackler and Reist, 2001), demonstrating that the density of glutamate receptors is unchanged. Because neither the area nor density of postsynaptic receptors is changed, the postsynaptic response to neurotransmitter release is unaltered in the mutants. Furthermore, the area of nc82 staining [polylysine motif mutants: 65,200 ± 7500; transgenic controls: 63,800 ± 7600 pixels at 40× (mean ± SEM)] is also not significantly different in the mutants ($p > 0.78$, Student's *t* test; n = 6 junctions for each genotype). Thus, the decrease in the evoked response in polylysine motif mutants likely results from a defect in vesicle availability or release probability, because it does not result from a decrease in the ability of the postsynaptic cell to respond to neurotransmitter nor a decrease in the active zone area.

The Calcium Cooperativity of Release Is Unchanged in the Polylysine Motif Mutants, but the Apparent Calcium Affinity of Release Is Decreased

During synaptic transmission, the amount of neurotransmitter release triggered by nerve stimulation depends on some power (n) of the extracellular Ca^{2+} concentration. In 1967, Dodge and Rahamimoff showed at frog neuromuscular junctions that the dependence of release on extracellular Ca^{2+} can be explained by assuming a cooperative action of ~4 Ca^{2+} ions (Dodge and Rahamimoff, 1967). Support for the hypothesis that the binding of three to five Ca^{2+} ions to a Ca^{2+} sensor(s) triggers neurotransmitter release has subsequently been demonstrated at other synapses as well, such as goldfish retinal bipolar synapses (Heidelberger *et al*., 1994), the rat Calyx of Held (Bollmann *et al*., 2000), and *Drosophila* neuromuscular junctions (Littleton *et al*., 1994; Stewart *et al*., 2000; Yoshihara and Littleton, 2002; Okamoto *et al*., 2005). To determine whether a disruption of Ca^{2+} binding by the polylysine motif mutant synaptotagmin contributed to the mutants' decreased release, we examined the Ca^{2+} dependence of release in both the polylysine motif mutants and the transgenic controls (Figure 3).

To estimate the Ca^{2+} dependence of release, we measured the mean EJP amplitude at various extracellular Ca^{2+} concentrations for both polylysine motif mutants and transgenic controls (Figure 3A). To examine the Ca^{2+} cooperativity of release, we graphed the mean EJP amplitude versus extracellular Ca^{2+} concentration on a double log plot (Figure 3B), and we determined that the slope for the polylysine motif mutants was 3.3 in nonsaturating Ca^{2+} ranges. This is similar to the cooperativity of 3.1 that was measured in our transgenic wild-type controls and to values (3.0–3.6) reported previously for *Drosophila* neuromuscular junctions (Littleton *et al*., 1994; Stewart *et al*., 2000; Yoshihara and Littleton, 2002; Okamoto *et al*., 2005). Thus, the polylysine motif mutation does not alter the number of Ca^{2+} ions necessary to trigger neurotransmitter release.

Although the Ca^{2+} cooperativity of release was not changed in the polylysine motif mutants, the EC_{50} was changed. To illustrate the increase in EC_{50} in the polylysine motif mutants, the EJP amplitudes were normalized to the predicted maximum value of the Hill equation for each genotype and replotted in Figure 3C [EC_{50} = 1.69 ± 0.08 mM for $-/-;P[syt^{KQ}]$ and EC_{50} = 1.20 ± 0.05 for $-/-;P[syt^{WT}]$ (mean ± SEM)]. Thus, the polylysine motif mutants exhibit an ~40% increase in EC_{50}. Because the cooperativity of release is unchanged in these mutants, the increase in EC_{50} corresponds to an ~40% decrease in the apparent Ca^{2+} affinity of release. Similar results have been reported for cultured, hippocampal neurons expressing synaptotagmin

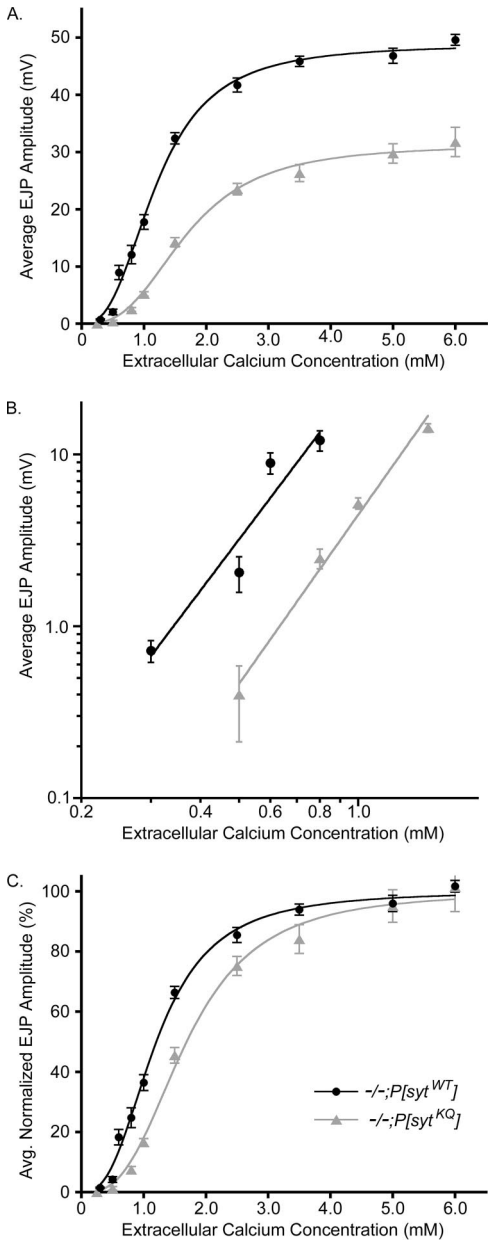

Figure 3. Calcium cooperativity of release is unchanged in the polylysine motif mutants, but the apparent calcium affinity and efficacy of release are decreased. EJPs were evoked by 0.05-Hz stimulation, and 10–15 sweeps were averaged for each fiber at each $[Ca^{2+}]$. (A) EJP amplitudes at various extracellular Ca^{2+} concentrations for both polylysine motif mutants (gray triangles), and transgenic controls (black circles). For both genotypes, at 0.3–0.6 mM extracellular $[Ca^{2+}]$, n = 5–15 fibers; at 1.5 mM extracellular $[Ca^{2+}]$, n = 34–42 fibers; and at all other extracellular $[Ca^{2+}]$, n = 15–32 fibers. (B) Mean EJP amplitudes versus extracellular Ca^{2+} concentration were graphed on a double log plot. The slope (n) was determined by fitting the data points with linear regression lines ($-/-;P[syt^{KQ}]$: n = 3.3, R = 0.99; $-/-;P[syt^{WT}]$: n = 3.1, R = 0.95). (C) EJP amplitudes in A were normalized to the maximum value predicted by the Hill equation for each genotype and replotted to illustrate the shift in EC_{50} ($-/-;P[syt^{KQ}]$: EC_{50} = 1.69 ± 0.08 mM; $-/-;P[syt^{WT}]$: EC_{50} = 1.20 ± 0.05 mM). Error bars are SEM.

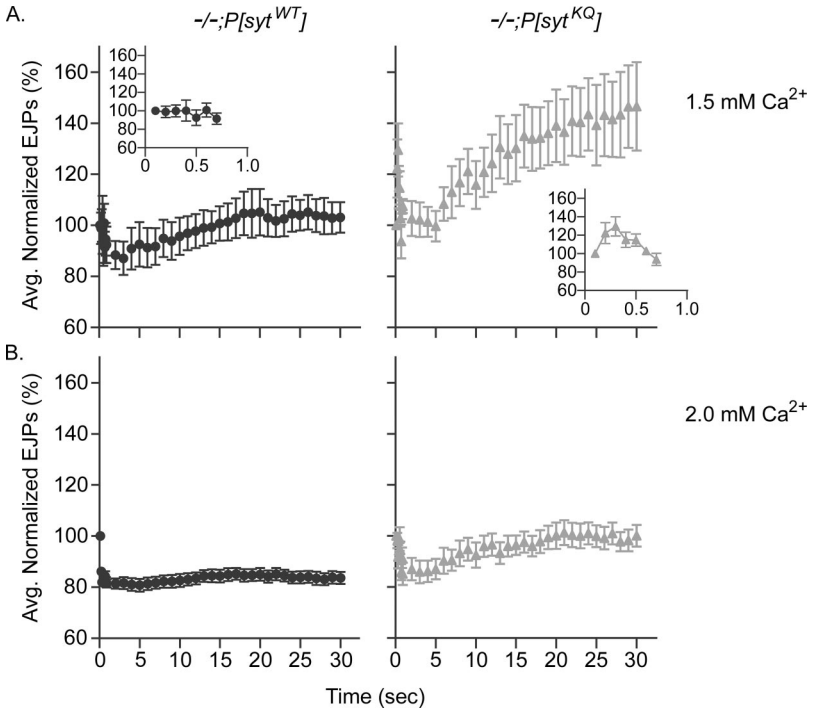

Figure 4. Polylysine motif mutants have a decreased release probability compared with transgenic controls. EJPs were evoked by 30 s of 10-Hz stimulation in 1.5 mM (A) or 2.0 mM (B) extracellular Ca^{2+}. EJP amplitudes were normalized to the amplitude of the EJP evoked by the first pulse and then averaged. After the first nine points, the points plotted are averages of 10 EJPs. Polylysine motif mutants: gray triangles, n = 6 fibers for 1.5 mM Ca^{2+} and n = 9 fibers for 2.0 mM Ca^{2+}. Transgenic controls: black circles, n = 6 fibers for 1.5 mM Ca^{2+} and n = 10 fibers for 2.0 mM Ca^{2+}. Error bars are SEM.

with a mutation in the polylysine motif (Borden *et al*., 2005; Li *et al*., 2006).

Synaptotagmin Polylysine Motif Mutants Have a Decreased Release Probability

The finding that the mutants exhibit less release at every Ca^{2+} concentration indicates that the polylysine motif mutants have a decreased release probability and/or a decrease in the number of readily releasable vesicles. To examine release probability, we measured synaptic facilitation and augmentation during high frequency stimulation. Although the mechanisms underlying short-term plasticity are not completely understood, generally a decrease in release probability results in greater synaptic augmentation and facilitation (Atwood and Karunanithi, 2002; Zucker and Regehr, 2002). EJPs were evoked by 10-Hz stimulation for 30 s. Polylysine motif mutants exhibited larger synaptic augmentation than transgenic control larvae in 1.5 mM extracellular Ca^{2+} (Figure 4A) and still exhibited synaptic augmentation at 2.0 mM extracellular Ca^{2+}, a concentration where control larvae no longer augment (Figure 4B). In addition, polylysine motif mutants exhibited facilitation during the first few pulses of 10 Hz stimulation in 1.5 mM Ca^{2+}, but transgenic control larvae did not (Figure 4A, insets). Examination of the Ca^{2+} concentration where evoked release failed in the mutants also indicates a decrease in release probability. At 0.5 mM extracellular Ca^{2+}, the failure rate in controls was 21 ± 5%, whereas that of the polylysine motif mutants was 64 ± 14% ($p < 0.05$). Thus, polylysine motif mutants exhibit a decreased release probability compared with transgenic control larvae.

The Readily Releasable Pool of Synaptic Vesicles Is Unaltered in Synaptotagmin Polylysine Motif Mutants

To determine whether there was also a change in the number of readily releasable vesicles, we elicited synaptic vesicle fusion with hypertonic sucrose. In *Drosophila* (Aravamudan *et al*., 1999; Suzuki *et al*., 2002a, b) as in frog (Fatt and Katz, 1952; Chen and Grinnell, 1997; Kashani *et al*., 2001) and in cultured neuronal cells (Stevens and Tsujimoto, 1995; Rosenmund and Stevens, 1996; Mochida *et al*., 1998), application of a hypertonic sucrose solution dramatically increases the frequency of miniature synaptic potentials. External Ca^{2+} is not needed for this response (Rosenmund and Stevens, 1996; Mochida *et al*., 1998; Suzuki *et al*., 2002a, b); however, the response is blocked when neuronal synaptobrevin (n-syb, also known as VAMP), SNAP-25, or syntaxin (syx) is cleaved by clostridial neurotoxin (Capogna *et al*., 1997), and it is greatly reduced in n-syb, syx, or Unc-13 *Drosophila* knockouts (Aravamudan *et al*., 1999). Thus, the hypertonic sucrose response is thought to bypass the Ca^{2+}-sensing step of vesicle fusion and to trigger the fusion of docked vesicles (Rosenmund and Stevens, 1996; Schikorski and Stevens, 2001) by using the same basic fusion machinery that underlies Ca^{2+}-triggered fusion. Furthermore, at *Drosophila* neuromuscular junctions, the size of the hypertonic response correlates with the size of the readily releasable pool of synaptic vesicles (Aravamudan *et al*., 1999; Suzuki *et al*., 2002a, b; Okamoto *et al*., 2005).

During a puff-application of 500 mM sucrose for 10 s, the frequency of miniature synaptic potentials (minis) dramatically increased in both polylysine motif mutants and transgenic controls (Figure 5). Figure 5A shows sample recordings from mutant and control larvae in both synaptic and nonsynaptic regions of the muscle fiber. The basal frequency of minis is elevated in each genotype only when sucrose is puffed on the synaptic region. The frequency before, during, and after the sucrose puff was determined and is plotted in Figure 5B. The basal frequency was higher in polylysine motif mutants than in controls (Figure 5B; Mackler and Reist, 2001). Therefore, to facilitate comparison between genotypes, the average frequency during the 10 s before the sucrose puff was subtracted from the calculated frequencies within each genotype (Figure 5C). The sucrose response in the polylysine motif mutants was comparable to that of controls. Thus, the decrease in the Ca^{2+}-evoked response recorded in the polylysine motif mutants (Figure 3) is not

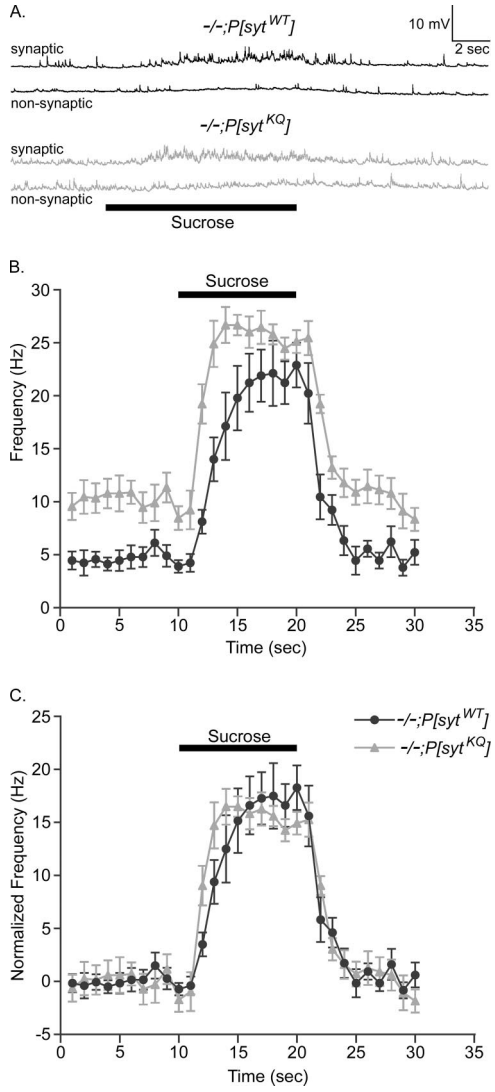

Figure 5. Size of the readily releasable pool of synaptic vesicles is unchanged in *synaptotagmin* polylysine motif mutants. (A) Sample traces showing that application of a hypertonic sucrose solution (bar) to synaptic regions for 10 s increases the frequency of miniature synaptic potentials. (B) Frequency of miniature synaptic potentials is plotted versus time from 10 s before to 10 s after the application of sucrose. (C) Because the basal rate of spontaneous release is greater in the mutants, the frequency of release was normalized to the basal rate within each genotype for comparison. The sucrose-induced, increased frequency in polylysine motif mutants (gray triangles, n = 9 fibers) is comparable to that in transgenic controls (black circles, n = 9 fibers). Error bars are SEM.

due to a decrease in the size of the readily releasable pool of synaptic vesicles (Figure 5), but rather to a decrease in the release probability (Figure 4).

The Polylysine Motif Mutation Slows Synaptotagmin·SNARE-mediated Lipid Mixing In Vitro

A decreased release probability could result from disruption of either Ca^{2+} sensing or synaptic vesicle docking/priming. The decrease in apparent Ca^{2+} affinity of release (Figure 3C) suggests a disruption in Ca^{2+} sensing. Yet, decreased Ca^{2+} affinity could only account for a decrease in the maximum amplitude of release (Figure 3A) if the Ca^{2+} affinity has decreased to such an extent that the intracellular Ca^{2+} concentration can never reach a level sufficient to trigger maximal release. Although at high extracellular Ca^{2+} concentrations, the Ca^{2+} influx through voltage-gated Ca^{2+} channels is expected to saturate (Hagiwara and Takahashi, 1967), at *Drosophila* neuromuscular junctions, this saturation is only reached when extracellular Ca^{2+} is $\geq$10 mM (Okamoto *et al*., 2005). Because the maximal response recorded in our polylysine motif mutants occurs around 5 mM (Figure 3A), well below saturation levels for Ca^{2+} channels, the decrease in maximal release recorded in these mutants is not due to the decrease in apparent Ca^{2+} affinity. Indeed, a decrease in the efficacy of release is more likely due to a disruption in the coupling of synaptotagmin to the release machinery (Borden *et al*., 2005).

On Ca^{2+} influx, the interaction of synaptotagmin with the presynaptic membrane is thought to be important for fusion (Bai *et al*., 2000, 2002; Wang *et al*., 2003; Rhee *et al*., 2005). The Ca^{2+}-independent interaction of the polylysine motif with t-SNARE heterodimers (Rickman *et al*., 2004) may play an important role in coupling synaptotagmin to the release machinery by positioning the Ca^{2+}-binding site of the C_2B domain near the plasma membrane. This Ca^{2+}-independent interaction would thus prime synaptic vesicles for efficient fusion. To directly test the importance of the C_2B polylysine motif in Ca^{2+}-independent facilitation of fusion, we examined the rate of fusion in a fluorescence lipid mixing assay. When v-SNARE–containing liposomes are mixed with liposomes containing t-SNARE heterodimers in the absence of Ca^{2+}, SNARE complex-specific fusion of the two populations occurred (Figure 6A; Weber *et al*., 1998; Parlati *et al*., 1999). Addition of membrane-bound synaptotagmin into the v-SNARE–containing liposomes directly accelerated the rate of fusion in a Ca^{2+}-independent manner (Figure 6, A and B; Mahal *et al*., 2002) consistent with the hypothesis that a Ca^{2+}-independent interaction between synaptotagmin and t-SNARE heterodimers facilitates SNARE-dependent fusion. Mutation of the polylysine motif, which has been shown to block the Ca^{2+}-independent interaction between synaptotagmin and t-SNARE heterodimers (Rickman *et al*., 2004), abolished the ability of synaptotagmin to accelerate the fusion reaction (Figure 6, A and B). These results indicate that the polylysine motif of synaptotagmin plays a critical role in Ca^{2+}-independent vesicle docking/priming and/or fusion in vitro.

Synaptic Vesicle Recycling Is Slowed in Polylysine Motif Mutants In Vivo

If the polylysine motif were important for synaptic vesicle docking/priming before Ca^{2+}-triggered fusion in vivo, then the polylysine motif mutants should exhibit a defect in synaptic vesicle availability, a process upstream of Ca^{2+} sensing. First, we investigated whether the polylysine motif functions in maintaining the supply of synaptic vesicles available for Ca^{2+}-triggered fusion by examining the ability of the mutants to sustain neurotransmitter release at the neuromuscular junction during high-frequency stimulation. When the rate of resupply is slower than the rate of synaptic vesicle exocytosis, the result is a net loss of synaptic vesicles available for release, which is reflected in decreasing EJP amplitudes. Thus, the degree of synaptic depression reflects the balance between synaptic vesicle exocytosis and synaptic vesicle resupply, which would include both synaptic vesicle mobilization and recycling (Delgado *et al*., 2000). Second, because recovery from synaptic depression occurs by synaptic vesicle recycling rather than vesicle mobilization from a reserve pool (Pyle *et al*., 2000; Richards *et al*., 2003), we

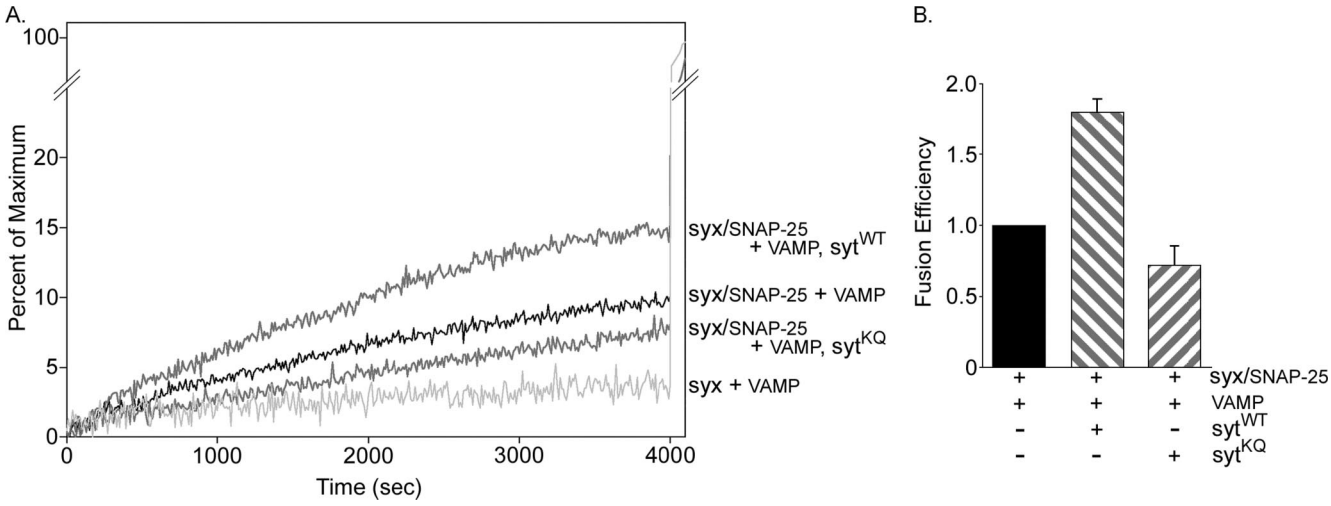

Figure 6. Polylysine motif mutation abolishes synaptotagmin's Ca^{2+}-independent ability to accelerate SNARE-mediated fusion. Fusion of v-SNARE liposomes (VAMP) with t-SNARE liposomes (syx/SNAP-25) was monitored via a fluorescence lipid mixing assay in the absence of Ca^{2+}. (A) Sample traces showing the increase in fluorescence when t-SNARE liposomes are mixed with v-SNARE liposomes that do not contain synaptotagmin (syx/SNAP-25 + VAMP), with v-SNARE liposomes that contain wild-type synaptotagmin (syx/SNAP-25 + VAMP, syt^{WT}) or with v-SNARE liposomes that contain the polylysine motif mutant synaptotagmin (syx/SNAP-25 + VAMP, syt^{KQ}). Light gray trace shows the background rate of lipid mixing when SNAP-25 is omitted from the t-SNARE liposomes (syx + VAMP). Detergent is added at 4000 s to determine the maximum fluorescence intensity (Weber *et al*., 2000). (B) The final values before the addition of detergent were used. After subtraction of background fusion (syx + VAMP), values were normalized to fusion in the absence of synaptotagmin and plotted as fusion efficiency. n = 3; error bars are SD.

investigated whether the polylysine motif functions specifically during synaptic vesicle recycling by examining the mutants' ability to recover from synaptic depression.

During 30 s of 10-Hz stimulation in 5 mM Ca^{2+}, the larval neuromuscular junction exhibited synaptic depression (Figure 7). Both the sample traces in Figure 7A and the averaged data graphed in Figure 7B illustrate that during 30 s of stimulation, evoked release decreased to a greater extent in polylysine motif mutants than in transgenic controls. To compare the magnitude of depression in mutant and control transgenic lines, EJP amplitudes were normalized to the EJP amplitude elicited by the first pulse in the train. Despite that the polylysine motif mutants have a decreased release probability and release fewer vesicles with each stimulus (Figure 3, 5 mM Ca^{2+}), they exhibited a small (~6%) increase in the magnitude of depression (Figure 7B). However, this apparent increase in synaptic depression might be an artifact of nonlinear summation. Because the EJP amplitudes are larger in the controls (Figures 3A and 7A), they would be more affected by nonlinear summation, which would underestimate their true degree of synaptic depression relative to the mutants. To explore this possibility, we applied the equation of Martin (1955) as an estimate to correct for nonlinear summation (our unpublished data). Indeed, using this correction factor, the polylysine motif mutants exhibited slightly less (~4%) synaptic depression than controls. However, because this formula is an imperfect correction (McLachlan and Martin, 1981), the true degree of synaptic depression is likely somewhere between that calculated from the noncorrected and corrected EJP amplitudes. Thus, the degree of synaptic depression is likely quite similar between mutants and controls.

Recovery from synaptic depression was examined either 5 or 15 s after the 30 s of 10-Hz stimulation ceased (Figure 7B). Only larvae that exhibited ≥95% recovery at an extended time point were included. Recovery from synaptic depression was dramatically slower in polylysine motif mutants than in transgenic controls. After 5 s, the mutants showed 41% less recovery than controls and by 15 s the mutants were still depressed 24%, whereas controls had already completely recovered. The slower rate of recovery in polylysine motif mutants in vivo demonstrates that a major defect caused by the polylysine motif mutation occurs during synaptic vesicle recycling before the Ca^{2+}-dependent fusion step; if a disruption of Ca^{2+}-dependent fusion were the primary defect in these mutants, they should recover from synaptic depression as quickly as controls. It also suggests that the polylysine motif functions in a Ca^{2+}-independent process, because Ca^{2+} levels drop rapidly upon the cessation of stimulation (within a few seconds; Wu and Betz, 1996; Karunanithi *et al*., 1997; Suzuki *et al*., 2000; Macleod *et al*., 2002).

Synaptic Vesicle Endocytosis Is Not Impaired in Polylysine Motif Mutants

Our in vitro studies demonstrate a Ca^{2+}-independent role for the polylysine motif in docking/priming and/or fusion, whereas our in vivo studies demonstrate a Ca^{2+}-independent role before Ca^{2+}-triggered fusion. Together, these studies support a role for the polylysine motif in docking/priming; however, they do not exclude additional disruptions during synaptic vesicle recycling. Recycling consists of many steps that include, but are not limited to, endocytosis, clathrin uncoating, refilling with neurotransmitter, docking, and priming of vesicles. Because functional studies demonstrate that synaptotagmin I is required during endocytosis (von Poser *et al*., 2000; Jarousse and Kelly, 2001; Jarousse *et al*., 2003; Poskanzer *et al*., 2003; Llinás *et al*., 2004; Nicholson-Tomishima and Ryan, 2004) and the polylysine motif of the C_2B domain of synaptotagmin is postulated to mediate this role (Takei and Haucke, 2001; but see Poskanzer *et al*., 2006), we wanted to determine whether endocytosis was disrupted in our mutants. However, the rate of endocytosis is difficult to assess in mutants with defects in exocytosis. Therefore, we investigated the importance of the C_2B polylysine motif for endocytosis by using three approaches.

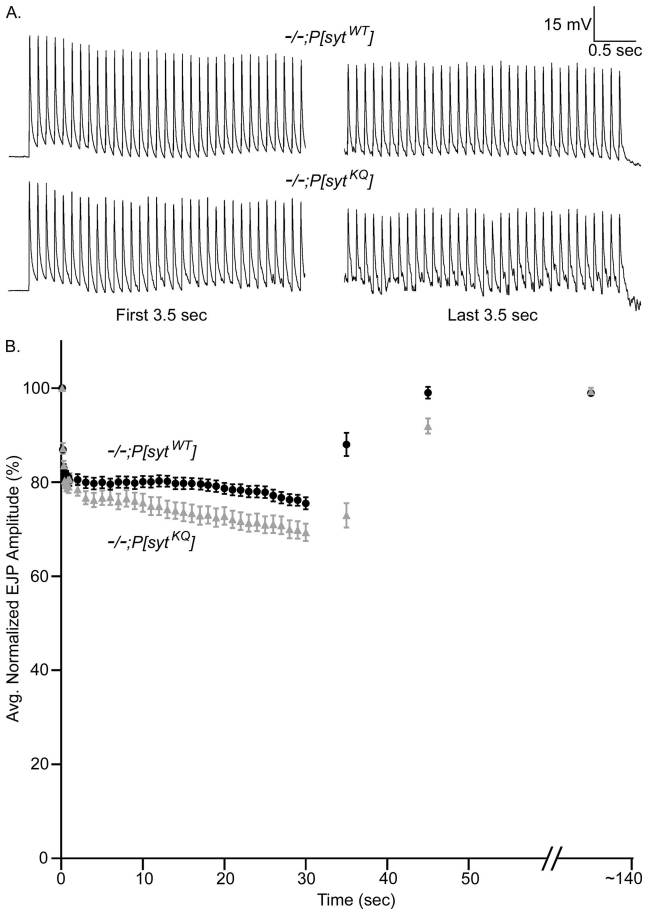

Figure 7. Polylysine motif mutants recover more slowly from synaptic depression than transgenic controls. Synaptic depression was elicited by stimulating fibers at 10 Hz for 30 s in 5 mM extracellular Ca^{2+}. Recovery was monitored by recording the EJP amplitude of a single shock either 5 or 15 s after the 10-Hz stimulation stopped. Each fiber was also stimulated at an extended time point (~140 s) to verify full recovery. (A) Representative traces from polylysine motif mutants ($-/-;P[syt^{KQ}]$) and transgenic controls ($-/-;P[syt^{WT}]$) showing the first and last 3.5 s of stimulation at 10 Hz for 30 s in saline containing 5 mM Ca^{2+}. (B) EJP amplitudes were normalized to the amplitude of the first shock. After the first nine points, the points plotted during the 10-Hz stimulation are averages of 10 EJPs. Transgenic controls: black circles, n = 10 fibers for 5-s recovery and n = 14 fibers for 15-s recovery. Polylysine motif mutants: gray triangles, n = 10 fibers for 5-s recovery and n = 14 fibers for 15-s recovery. Error bars are SEM.

As a first step in examining endocytosis, the ability of the mutants to maintain a supply of synaptic vesicles for release was further challenged by stimulating preparations at 10 Hz for 4 min in 5 mM Ca^{2+}. The averaged data (Figure 8A) illustrate that during the 4 min of stimulation evoked release decreased to a greater extent in polylysine motif mutants than in transgenic controls. To compare the magnitude of depression in mutant and control transgenic lines, EJP amplitudes were binned at 5-s intervals and normalized to the first EJP amplitude bin (Figure 8B). EJP amplitudes from polylysine motif mutants did decrease to a greater extent than the transgenic controls. Although this result seems to suggest that the rate of synaptic vesicle resupply relative to the rate of exocytosis is slowed in the polylysine motif mutants compared with controls, again this apparent difference is probably exaggerated by nonlinear summation. Indeed, when the correction factor of Martin (Martin, 1955) is applied, the polylysine motif mutants again show less depression (~4%) than controls (our unpublished data). Even without the correction factor, the increased synaptic depression in the polylysine motif mutants is not severe (5% more depression after 60 s and 15% more after 4 min). Thus, the polylysine motif mutants are able to maintain release relatively well for at least 4 min of 10-Hz stimulation, an unexpected result if the polylysine motif were critical for endocytosis.

A common ultrastructural phenotype seen at neuromuscular junctions in endocytic mutants is severe synaptic vesicle depletion (Koenig *et al*., 1989; Fernandez *et al*., 1998; Verstreken *et al*., 2002, 2003). Indeed, syt^{null} mutants in *Drosophila* exhibit such depletion, along with an accumulation of larger membranous structures (Figure 9, bottom; Reist *et al*., 1998; Loewen *et al*., 2006). Therefore, our second approach was to examine the synaptic ultrastructure of polylysine motif mutants to see whether they exhibited synaptic vesicle depletion, indicative of an endocytic defect.

The boutons of transgenic control larvae (Figure 9, top) and polylysine motif mutants (Figure 9, middle) contain numerous synaptic vesicles located at active zones and throughout the nerve terminal, and no accumulation of larger membranous structures (compare to syt^{null} mutants, Figure 9, bottom). Thus, both the polylysine motif mutant transgene and the wild-type transgene are able to *rescue* the ultrastructural deficits seen in syt^{null} mutant terminals. Again, this finding suggests that the polylysine motif of synaptotagmin does not mediate the role of synaptotagmin in synaptic vesicle endocytosis. Furthermore, it is consistent with our finding that the readily releasable pool size is not changed in polylysine motif mutants (Figure 5).

Finally, to examine the rate of endocytosis in polylysine motif mutants directly, we used an FM 1-43 dye uptake assay. FM 1-43 fluoresces when it inserts into lipid membranes. If it is present when synaptic vesicle membrane is internalized, these synaptic vesicles will be fluorescently labeled. Subsequently, the dye can be washed from the outside of cells, leaving only the internalized synaptic vesicles labeled. Thus, FM 1-43 makes it possible to examine the process of endocytosis directly (Betz *et al*., 1992).

Figure 10A illustrates the endocytic assay we used to test the involvement of the polylysine motif in endocytosis [adapted from the assays of (Ryan *et al*., 1996; Kuromi and Kidokoro, 1998; Stimson *et al*., 2001; Kim *et al*., 2002)]. *Drosophila* third instars were stimulated for 6 min with a stimulating saline containing high potassium. Stimulation was terminated when the stimulating saline was replaced by standard saline plus 3 μM TTX. TTX was included to block any spontaneous action potentials coming from the attached CNS. The standard saline + TTX was left on the preparation for a variable amount of time (Δt = 0, 30, 60, or 180 s). After Δt, the preparation was bathed in standard saline containing TTX and FM 1-43 for 6 min to label endocytosing vesicles. Finally the preparation was washed for 15 min with 3 changes of Ca^{2+}-free saline to remove extracellular FM 1-43 from the plasma membrane. Ca^{2+}-free saline was used to minimize vesicle fusion during the washing stage. After washing, the fluorescence intensity of the FM 1-43-labeled synaptic boutons was measured.

Because FM 1-43 is present after stimulation ceases, and the signal is subsequently normalized to its maximum (see below), the above-mentioned protocol allowed us to determine the rate of internalization independent of the rate of exocytosis (Ryan *et al*., 1996; Stimson *et al*., 2001; Kim *et al*., 2002). However, only those synaptic vesicles that remain on

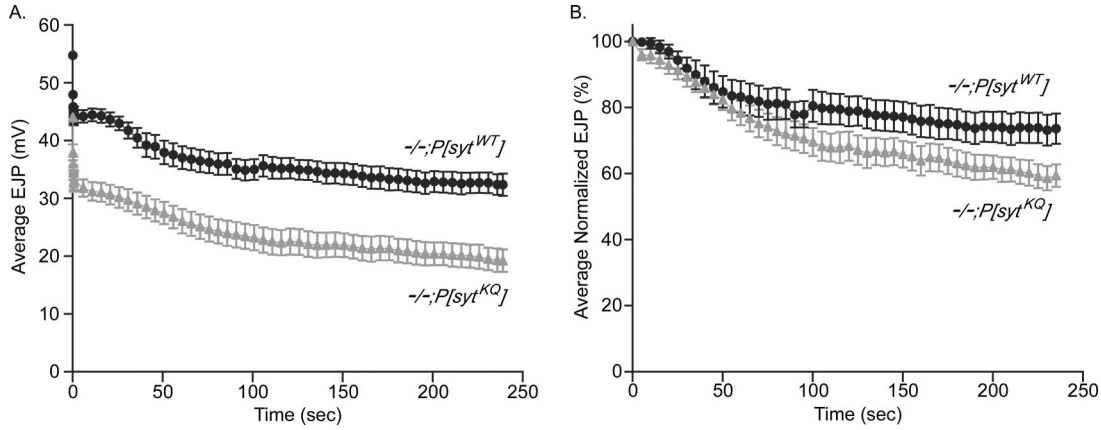

Figure 8. Polylysine motif mutants maintain significant levels of evoked release during prolonged high-frequency stimulation. (A) Average EJP amplitudes evoked during 4 min of 10-Hz stimulation in saline containing 5 mM Ca^{2+}. Except for the first nine points and the last point, the EJP amplitudes were binned at 5-s intervals, and the average of the bin is plotted. The first nine points are not binned. The last point is the average EJP amplitude of a 3-s bin. Transgenic controls: black circles, n = 8 fibers. Polylysine motif mutants: gray triangles, n = 10 fibers. (B) Same EJP amplitudes as in A but binned at 5-s intervals and normalized to the first 5-s bin.

the surface at the end of the stimulation can be labeled. Thus, a strong stimulus was needed to provide sufficient fluorescent signals for analysis. In standard saline containing 1.5 mM Ca^{2+}, evoked release is only 14.2 ± 0.82 mV in the polylysine mutants (Figures 1B and 3A) and the FM 1-43 labeling achieved by the above-mentioned protocol was quite dim. Because our goal in these experiments was to determine whether endocytosis is a major defect in the polylysine motif mutants, we increased the Ca^{2+} in the stimulating saline to 5 mM to maximize release in these mutants and thus to increase FM 1-43 labeling.

During the delay period between the end of stimulation and addition of FM 1-43 dye, Δt, some fraction of the synaptic vesicle membrane remaining on the plasma membrane undergoes endocytosis. As Δt increases, more and more vesicle membrane is internalized, leaving less vesicle membrane on the surface to be labeled when FM 1-43 is subsequently applied. Therefore, as Δt increases, less FM 1-43 is internalized and nerve terminal labeling becomes progressively dimmer. This is illustrated in Figure 10B, which shows FM 1-43-labeled synaptic boutons on muscle 6 and 7 in both transgenic control and polylysine motif mutant lar-

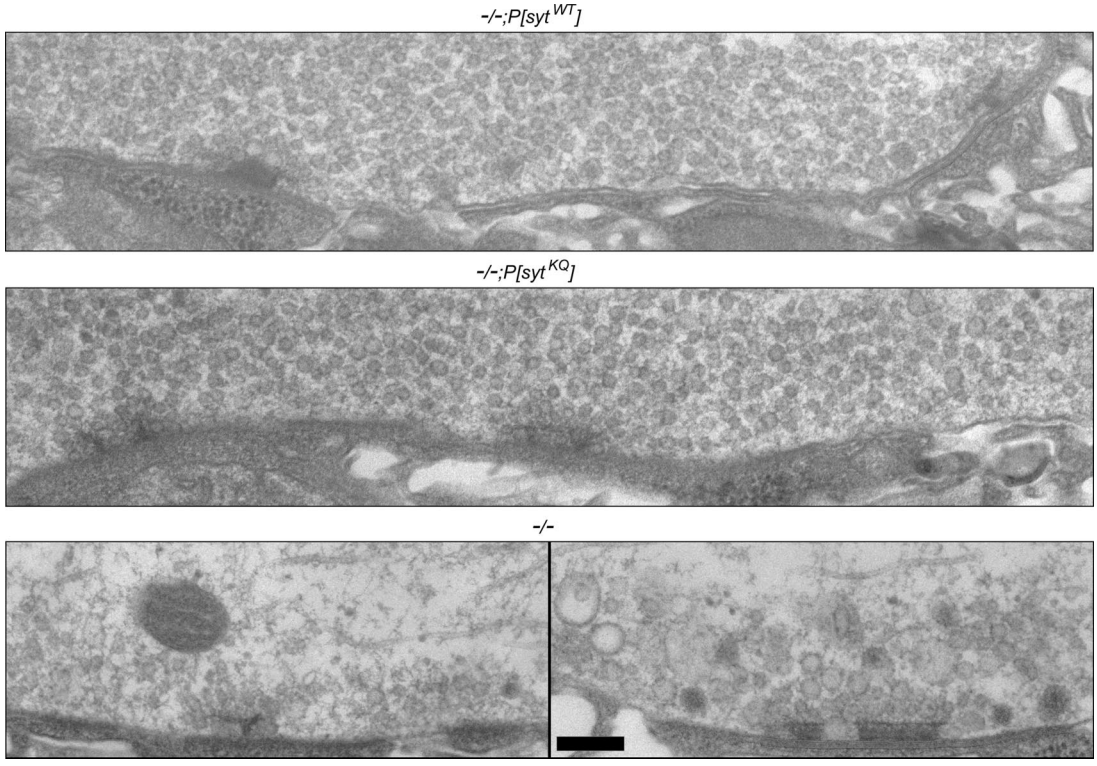

Figure 9. Synaptic vesicles are abundant in nerve terminals of polylysine motif mutants. Electron micrographs showing the synaptic ultrastructure of neuromuscular junctions in transgenic controls (top), polylysine motif mutants (middle), and syt^{null} mutants (bottom). Bar, 200 nm.

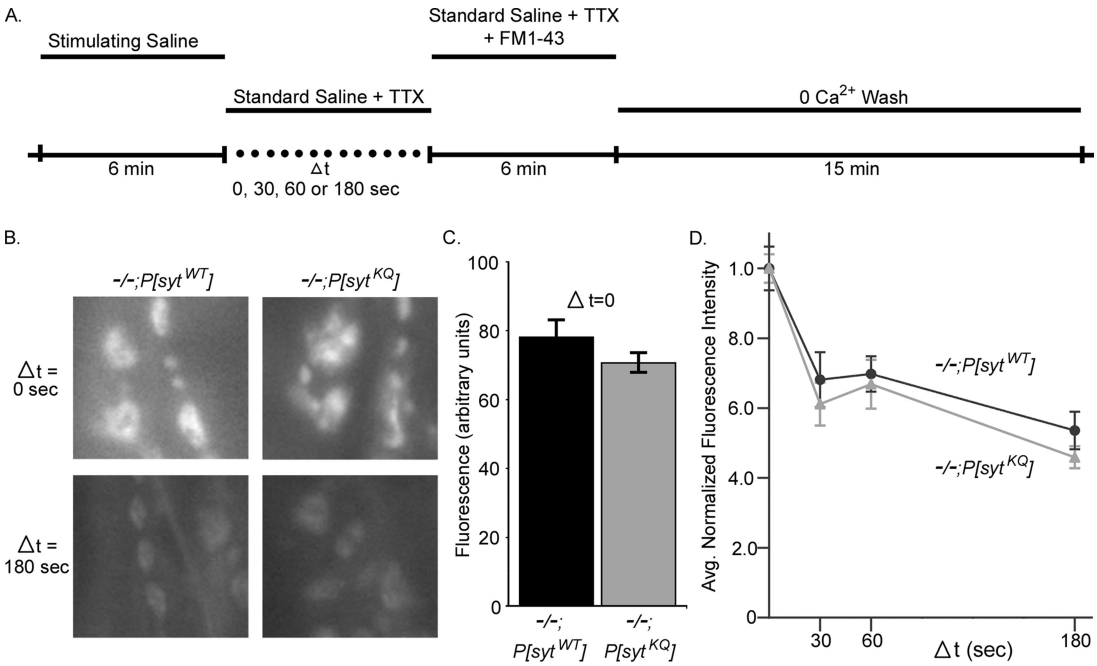

Figure 10. Rate of endocytosis is not significantly different in *synaptotagmin* polylysine motif mutants. (A) Schematic of endocytic assay using FM 1-43 dye. (B) Synaptic boutons on muscle 6 and 7 in polylysine motif mutants (−/−;*P*[syt^{KQ}]) and transgenic controls (−/−;*P*[syt^{WT}]) were labeled with FM 1-43 dye as described in A. Labeling is shown for $\Delta t = 0$ s (top) and $\Delta t = 180$ (bottom). (C) At $\Delta t = 0$, the average fluorescence intensity of boutons from polylysine motif mutants was ~10% less than controls. (D) Fluorescence intensity of synaptic boutons is graphed as a function of the time between stimulus termination and application of the FM 1-43 dye (Δt). Polylysine motif mutants: gray triangles, n = 132–135 boutons from nine larvae for each Δt. Transgenic controls: black circles, n = 135 boutons from nine larvae for each Δt. To account for differences between genotypes in the absolute number of synaptic vesicles released during stimulation, fluorescence values for each genotype were normalized to the fluorescence intensity of that genotype at $\Delta t = 0$ s. 95% CI = −11.6 to 2.75.

vae after $\Delta t = 0$ and 180 s. In both polylysine motif mutant and transgenic control larvae, labeling was brightest at $\Delta t = 0$ s and dimmest at $\Delta t = 180$ s. Loading was dependent on both stimulation and Ca^{2+} (our unpublished data).

At all time points, the mean fluorescence of polylysine motif mutant boutons was somewhat lower than the mean fluorescence for controls. This is most likely because the mutants exocytose fewer vesicles than the controls during the stimulation. Figure 10C shows the mean level of FM 1-43 labeling at $\Delta t = 0$ s for both mutants and controls. Under these stimulation conditions (high K^+, high Ca^{2+} for 6 min), the amount of membrane awaiting endocytosis after stimulation ceased was only ~10% less in the polylysine motif mutants. Because exocytosis is ~40% less in the mutants in 5 mM Ca^{2+} (Figure 3A), this relative buildup of vesicle membrane stranded in the plasma membrane could indicate that endocytosis is slowed in the mutants. However, a single time point cannot accurately measure the rate of endocytosis because other factors, such as the size of the releasable pools and saturation of the endocytic machinery, can also influence the amount of membrane awaiting endocytosis. So, to determine the kinetics of synaptic vesicle internalization independent of this ~10% difference, we normalized our data according to previous methods used to compare endocytic rates between preparations with different amounts of exocytosis (Ryan *et al*., 1996; Stimson *et al*., 2001; Kim *et al*., 2002). Thus, the fluorescence value of each bouton was normalized to the mean fluorescence value of boutons of the corresponding genotype at $\Delta t = 0$ s.

If the rate of endocytosis were impaired in polylysine motif mutant larvae, then during any given Δt, they should not be able to endocytose as large a fraction of the remaining synaptic vesicle membrane as controls. As a result, a larger proportion of synaptic vesicle membrane would remain in the plasma membrane when the FM 1-43 was applied, leading to proportionally more FM 1-43 internalization. Thus, if polylysine motif mutants had endocytic deficits, then after any given Δt, polylysine motif terminals should exhibit a normalized fluorescence that was brighter than controls. Indeed, *stoned* mutants, which also exhibit a decrease in evoked release, were shown to have an endocytic defect using a similar assay (Stimson *et al*., 2001). C_2B polylysine motif mutants, in contrast, do not (Figure 10D). At each time point, the normalized fluorescence of the mutant terminals was slightly lower than that of controls. Lower fluorescence values would suggest a faster rate of endocytosis in the mutants, not an impaired rate. However, the differences between polylysine motif mutants and transgenic controls were not statistically significant. The mixed model ANOVA used to generate a 95% confidence interval for the true difference between mutants and controls included 0 (−11.6, 2.75). Because the rate of endocytosis was not disrupted in the mutants, the relatively small difference in labeling at $\Delta t = 0$ s (Figure 10C) suggests that endocytosis was the rate-limiting step and that our strong stimulation protocol successfully drove the majority of the cycling vesicle membrane (which is approximately equal in mutants and controls; Figure 5C) to the surface.

DISCUSSION

The highly conserved C_2B polylysine motif plays a functional role in the synaptic vesicle cycle. Mutations in this motif decrease the amplitude of the evoked response at all

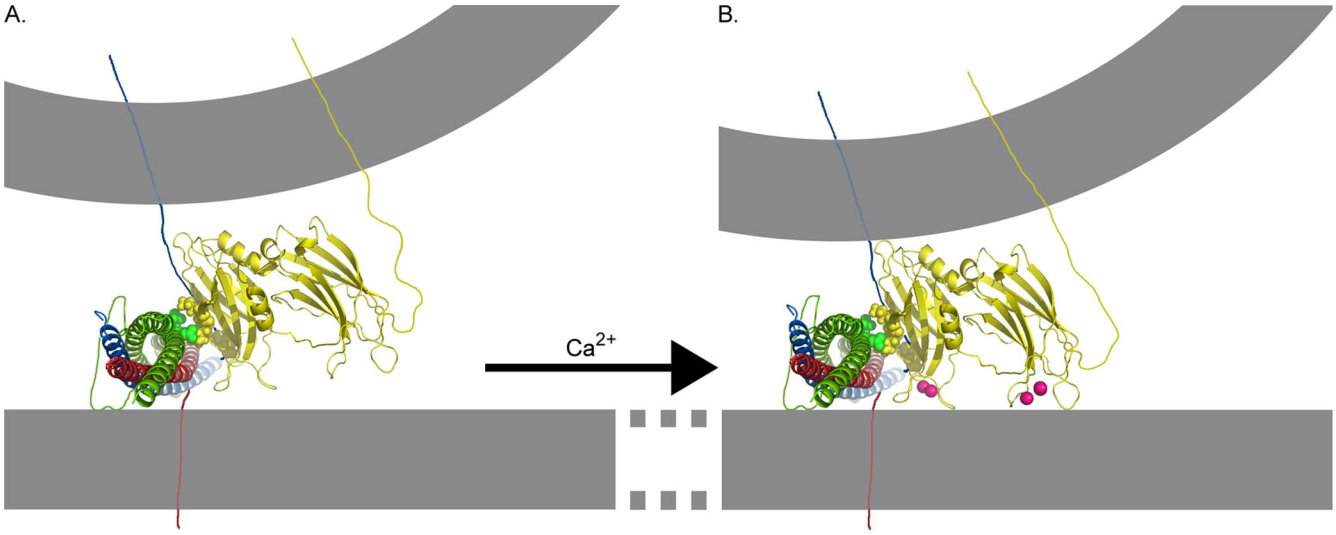

Figure 11. Model of the role of the polylysine motif in Ca^{2+}-independent synaptic vesicle docking/priming. Nuclear magnetic resonance structures of C_2A (PDB file 1BYN) and C_2B (PDB file 1K5W) domains (yellow) of synaptotagmin, the crystal structure of the core complex (PDB file 1SFC, containing VAMP [blue], SNAP-25 [green], and syntaxin [red]), and Ca^{2+} (pink) are shown to scale by using the PyMOL Molecular Graphics System (DeLano, 2002). The N termini of the SNARE proteins are darker and the C termini are paler to indicate depth. The membranes, the link between C_2A and C_2B domains of synaptotagmin, as well as transmembrane links for synaptotagmin, VAMP, syntaxin, and SNAP-25 were subsequently added. (A) Ca^{2+}-independent interactions between the polylysine motif lysines in C_2B (yellow, space-filled residues) with negatively charged residues of SNAP-25 (green, space-filled residues; Rickman *et al*., 2004, 2006) could hold the C_2B Ca^{2+} binding site in the immediate vicinity of negatively charged phospholipids of the presynaptic membrane. (B) On Ca^{2+} influx, Ca^{2+}-binding pockets of synaptotagmin insert into the plasma membrane (Bai *et al*., 2000, 2002, Wang *et al*., 2003; Rhee *et al*., 2005) allowing these negatively charged phospholipids to complete the coordination sphere for Ca^{2+} (Fernández-Chacón *et al*., 2002). The opposite end of the C_2B domain interacts with the vesicle membrane (Araç *et al*., 2006) pulling the vesicle and plasma membranes closer together.

Ca^{2+} concentrations; increase the EC_{50} of Ca^{2+} for release; increase augmentation, facilitation, and failure rate at low Ca^{2+} concentrations; cause a marked decrease in the rate of recovery from synaptic depression; block Ca^{2+}-independent interactions with t-SNARE heterodimers (Rickman *et al*., 2004); and abolish the ability of synaptotagmin to accelerate Ca^{2+}-independent, SNARE-mediated fusion. However, polylysine motif mutations do *not* alter postsynaptic receptor area, the size of minis (Mackler and Reist, 2001), active zone area, the Ca^{2+} cooperativity of release, the size of the hypertonic response, or the rate of endocytosis, and they do not result in synaptic vesicle depletion. These findings are discussed in terms of a single deficit hypothesis, namely, disruption of Ca^{2+}-independent synaptic vesicle docking/priming (Figure 11).

Neither the response to a single quantum of neurotransmitter (Mackler and Reist, 2001) nor the area occupied by the postsynaptic receptors has decreased. Therefore, the postsynaptic responsiveness is unchanged and the decrease in the evoked response must be due to a presynaptic deficit; either the size of the readily releasable pool and/or the release probability of synaptic vesicles must be decreased in the polylysine motif mutants. Because neither the area of presynaptic active zones nor the response to a hypertonic solution is decreased, the size of the readily releasable pool has not changed in the mutants. Together with the finding that facilitation, augmentation, and failure rate are increased in the mutants, these data provide strong support for the hypothesis that the polylysine motif regulates the release probability of synaptic vesicles.

Of the previously hypothesized functions for the polylysine motif, a decrease in either Ca^{2+}-triggered fusion and/or Ca^{2+}-independent docking/priming could result in a decrease in vesicle release probability. We discuss each possibility in turn below.

Although a defect in Ca^{2+}-triggered fusion could result in a decrease in release probability, it cannot account for all of the deficits seen in polylysine motif mutants. Ca^{2+}-dependent binding to negatively charged phospholipids (PC/PS) is reportedly unchanged by a polylysine motif mutation when a GST-pull-down assay is used (Bai *et al*., 2004), suggesting that Ca^{2+} sensing is not disrupted by this mutation in vitro. However, recent results using a centrifugation assay and PC/PE/PS/PI (phosphatidylinositol)/cholesterol lipids suggest otherwise (Li *et al*., 2006). In our polylysine motif mutants, the apparent Ca^{2+} affinity of release has decreased, suggestive of a Ca^{2+}-sensing defect. However, the mutants exhibit their maximal response at a Ca^{2+} concentration well below the level thought to saturate Ca^{2+} channels (Okamoto *et al*., 2005). Therefore, the decrease in maximal response cannot be fully accounted for by the decrease in the apparent Ca^{2+} affinity. Instead, the decrease in maximal response suggests that the decrease in release probability is due to disrupted coupling between the mutant synaptotagmin and the release machinery (Borden *et al*., 2005). Although disrupted coupling could disrupt fusion, our data demonstrate that the polylysine motif must play a role in the synaptic vesicle cycle at a step other than fusion. If the primary defect in the polylysine motif mutants were in Ca^{2+}-triggered fusion, then the mutants should recover from synaptic depression as quickly as controls, but they do not. Recovery from depression is dramatically slower in mutants than in controls. Thus, the defect in the polylysine motif mutants cannot be solely in the Ca^{2+}-triggered fusion step.

In contrast, a defect in Ca^{2+}-independent docking/priming can account for all of the deficits seen in the polylysine motif mutants, even the decrease in the apparent Ca^{2+} affinity of release. It has been shown that negatively charged phospholipids increase the apparent Ca^{2+} affinities of the C_2 domains of synaptotagmin by completing the coordination

spheres for Ca^{2+} (Fernández-Chacón *et al*., 2001). It may be that the Ca^{2+}-independent interaction between the C_2B polylysine motif and t-SNARE heterodimers primes vesicles for Ca^{2+}-triggered fusion by positioning the C_2B Ca^{2+}-binding pocket near the negatively charged phospholipids of the presynaptic membrane (Figure 11A). Thus, upon Ca^{2+} influx, these lipids are immediately at hand to complete the coordination sphere of calcium (Figure 11B), thereby effectively increasing the affinity of synaptotagmin for Ca^{2+}. It should be noted that the Ca^{2+}-independent interaction between the polylysine motif and PIP_2-containing membranes could also mediate such a function (Bai *et al*., 2004). The decreased affinity in the polylysine motif mutants (Figure 3; Borden *et al*., 2005; Li *et al*., 2006) may result from the lack of a Ca^{2+}-independent interaction that normally strengthens Ca^{2+}-dependent phospholipid binding. Thus, although our data do not preclude a defect in Ca^{2+} sensing, direct disruption of Ca^{2+} binding is not required to account for the decrease in Ca^{2+} affinity seen in the polylysine motif mutants.

Further evidence in support of the hypothesis that the polylysine motif mediates Ca^{2+}-independent docking/priming comes from our experiments where we monitored recovery from synaptic depression. The ability of the mutants to maintain neurotransmitter release during 30 s of high-frequency stimulation is less affected than their ability to recover from this synaptic depression (Figure 7). This difference may be because intracellular Ca^{2+} is higher during stimulation compared with after stimulation (Wu and Betz, 1996; Karunanithi *et al*., 1997; Suzuki *et al*., 2000; Macleod *et al*., 2002). Elevated intracellular Ca^{2+} during a stimulus train is thought to accelerate the rate of recovery from synaptic depression during the train compared with the rate of recovery poststimulation (Zucker and Regehr, 2002). Our observation that the polylysine motif mutants have greater difficulty recovering from depression (when intracellular Ca^{2+} levels have fallen) than maintaining neurotransmitter release (when intracellular Ca^{2+} levels are elevated) also indicates that the defect in these mutants is in a Ca^{2+}-independent process. This finding suggests that during the stimulus train, Ca^{2+}-dependent processes that are not impaired by the mutation may partially rescue the Ca^{2+}-independent defect.

We provide direct support for the hypothesis that Ca^{2+}-independent docking/priming is impaired in polylysine motif mutants with our finding that the mutation abolished the Ca^{2+}-independent ability of synaptotagmin to accelerate the fusion of v-SNARE–containing vesicles to t-SNARE heterodimer-containing vesicles (Figure 6). Other in vitro studies also support this hypothesis. The C_2B polylysine motif exhibits Ca^{2+}-independent interactions with t-SNARE heterodimers (Rickman *et al*., 2004), suggesting that the polylysine motif may dock vesicles by bringing the synaptic vesicle v-SNARE into proximity with the t-SNAREs (Rickman *et al*., 2004, 2006). Such an interaction could also prime vesicles by positioning the C_2B Ca^{2+}-binding pocket near the presynaptic membrane, thereby facilitating Ca^{2+}-triggered fusion (Figure 11). Ca^{2+}-independent docking/priming by the polylysine motif could also be mediated by its Ca^{2+}-independent interaction with PIP_2 (Bai *et al*., 2004), which is located predominately in the plasma membrane (Holz *et al*., 2000; Micheva *et al*., 2001). This interaction may facilitate a *trans*-interaction between synaptotagmin in the synaptic vesicle membrane and PIP_2 in the plasma membrane. This Ca^{2+}-independent interaction has been proposed to mediate docking/priming of vesicles because it increases the rate of Ca^{2+}-dependent penetration of synaptotagmin into lipid membranes (Bai *et al*., 2004), a step thought to be important for fusion. Alternatively, a very recent report indicates that the polylysine motif does not increase the rate of vesicle fusion, but instead increases the number of vesicles capable of fusing with a fast time constant (Li *et al*., 2006). This finding is consistent with the polylysine motif facilitating synaptic vesicle docking/priming. In this scenario, the polylysine motif mutation would result in fewer synaptic vesicles existing in a fully primed state. Fewer primed synaptic vesicles could explain the selective decrease in the amount of fast release (Li *et al*., 2006), and the decreased release probability (Figure 4; Borden *et al*., 2005; Li *et al*., 2006) seen in polylysine motif mutants. Furthermore, if the polylysine motif did indeed facilitate synaptic vesicle priming, then priming would be slower in its absence, and recovery from synaptic depression would be slower in polylysine motif mutants (Figure 7). Thus, disruption of either of these interactions (with t-SNARE heterodimers, as indicated by Figure 6, or with PIP_2) could impair Ca^{2+}-independent docking/priming while leaving many interactions proposed to mediate Ca^{2+}-dependent docking/priming intact (Augustine, 2001).

Ultrastructural studies have demonstrated that synaptotagmin is important for synaptic vesicle docking. In *synaptotagmin* null mutants, the number of morphologically docked vesicles is specifically decreased (Reist *et al*., 1998; Loewen *et al*., 2006). A detailed ultrastructural analysis would be required to determine whether the C_2B polylysine motif participates in the function of synaptotagmin in vesicle docking. However, in random electron micrographs of neuromuscular junctions from transgenic controls (Loewen *et al*., 2006) and polylysine motif mutants (our unpublished data), vesicles located immediately adjacent to the presynaptic membrane are common, unlike *synaptotagmin* null mutants (Reist *et al*., 1998; Loewen *et al*., 2006). In addition, because the readily releasable pool maybe correlated with the number of docked synaptic vesicles (Rosenmund and Stevens, 1996; Schikorski and Stevens, 2001), our observation that the readily releasable pool is unchanged would be consistent with no disruption in synaptic vesicle docking. Thus, although we cannot exclude vesicle docking, it is more likely that the polylysine motif functions primarily after docking to prime vesicles for rapid, efficient fusion upon the influx of Ca^{2+}.

The marked slowing of recovery from synaptic depression after high-frequency stimulation demonstrates that the polylysine motif is necessary for a membrane trafficking step of the synaptic vesicle cycle in vivo. Although our in vitro data demonstrate a role for the polylysine motif in Ca^{2+}-independent docking/priming, they do not exclude additional defects such as in endocytosis. However, further analysis of our mutants ruled out a major role for the polylysine motif in synaptic vesicle endocytosis. Electrophysiological, ultrastructural, and FM 1-43 studies are all inconsistent with the hypothesis that the polylysine motif functions during endocytosis. In known endocytic mutants (e.g., synaptojanin and endophilin), evoked release during low-frequency stimulation is not different from controls. However, during 4 min of 10-Hz stimulation, these mutants exhibit severe synaptic depression (Verstreken *et al*., 2002, 2003). In contrast, polylysine motif mutants have a significant defect in evoked release during low frequency stimulation (Figures 1 and 3; Mackler and Reist, 2001; Borden *et al*., 2005; Li *et al*., 2006), yet they exhibit only modest if any increase in synaptic depression during 4 min of 10-Hz stimulation (Figure 8). Thus, the electrophysiological phenotype of the polylysine motif mutants is inconsistent with an endocytic defect.

Ultrastructural analysis of nerve terminals in endocytic mutants show severe synaptic vesicle depletion (Koenig *et al*., 1989; Fernandez *et al*., 1998; Guichet *et al*., 2002; Verstreken *et al*., 2002, 2003). Indeed, syt^{null} mutants in *Drosophila* and *Caenorhabditis elegans* also show severe synaptic vesicle depletion (Figure 9, bottom; Jorgensen *et al*., 1995; Reist *et al*., 1998; Loewen *et al*., 2006), consistent with the role of synaptotagmin in endocytosis (von Poser *et al*., 2000; Jarousse and Kelly, 2001; Jarousse *et al*., 2003; Poskanzer *et al*., 2003; Llinás *et al*., 2004; Nicholson-Tomishima and Ryan, 2004). However, nerve terminals in polylysine motif mutants do not exhibit synaptic vesicle depletion (Figure 9, middle). On the contrary, the polylysine motif mutant *synaptotagmin* transgene rescues the syt^{null} ultrastructural phenotype, again inconsistent with an endocytic defect.

We directly measured the rate of synaptic vesicle internalization in polylysine motif mutants and controls using an FM 1-43 assay and found that it was not significantly different (Figure 10D). Previous studies indicate that the rate of endocytosis may decrease as more and more membrane is internalized (Wu and Betz, 1996; Sankaranarayanan and Ryan, 2001). Thus, the trend toward faster internalization in the polylysine motif mutants may be due to the fact that they have ~10% less membrane to endocytose after stimulation than do their controls; the boutons of polylysine motif mutants are ~90% as bright as control boutons at $\Delta t = 0$ (Figure 10C).

The finding that polylysine motif mutants have only ~10% less membrane to endocytose than controls at $\Delta t = 0$ (Figure 10C), whereas their evoked release is ~40% less in 5 mM Ca^{2+} (Figure 3A), may seem in conflict with our finding that endocytosis is not disrupted. However, that endocytosis is much slower than exocytosis and our finding that the size of the readily releasable vesicle pool is similar in polylysine motif mutants and controls (Figure 5B) could account for this apparent discrepancy. If the strong stimulation protocol used in the dye uptake assay (90 mM K^+ and 5 mM Ca^{2+} for 6 min) fully mobilized the readily releasable pool in both genotypes and endocytosis were the rate limiting step, then when stimulation stopped a major fraction of the cycling membrane in both genotypes would remain incorporated in the plasma membrane awaiting endocytosis. Because evoked release is decreased in polylysine motif mutants, it is likely that for the mutants, the total time required to fully mobilize the readily releasable pool would be longer than for controls. However, if this time were <6 min, then at $\Delta t = 0$ both genotypes would have fully mobilized their readily releasable pool. Because the size of this pool is similar in both genotypes (Figure 5B), both would have similar amounts of vesicle membrane awaiting endocytosis at $\Delta t = 0$.

Multiple studies have indicated a functional role for synaptotagmin I in synaptic vesicle endocytosis in vivo (Figure 9, bottom; Jorgensen *et al*., 1995; Reist *et al*., 1998; Poskanzer *et al*., 2003; Llinás *et al*., 2004; Nicholson-Tomishima and Ryan, 2004; Loewen *et al*., 2006). Whereas the C_2B domain has been implicated in endocytic function of synaptotagmin (Jarousse and Kelly, 2001; Littleton *et al*., 2001; Jarousse *et al*., 2003; Llinás *et al*., 2004), our studies clearly demonstrate that the polylysine motif within the C_2B domain is not involved. Our results do not, however, rule out a role for other motifs within the C_2B domain of synaptotagmin in synaptic vesicle endocytosis. Indeed, the conserved WHXL motif in the C_2B domain of synaptotagmin has been shown to be critical for internalization of synaptotagmin in PC12 cells (Jarousse *et al*., 2003).

Three molecular mechanisms have been proposed to mediate the role of the polylysine motif in the synaptic vesicle cycle: 1) synaptic vesicle endocytosis, 2) regulation of Ca^{2+}-triggered fusion, and 3) Ca^{2+}-independent docking and/or priming of synaptic vesicles. Our data demonstrate that the polylysine motif mutation decreases the release probability of synaptic vesicles. Electron micrographs show that the polylysine motif mutant larvae do not exhibit synaptic vesicle depletion and an FM 1-43 assay demonstrates that the rate of endocytosis is not impaired in these mutants. The mutant larvae maintain release relatively well during high-frequency stimulation when Ca^{2+} levels are elevated. However, they are slow to recover from synaptic depression, when intracellular Ca^{2+} levels are low, indicating that a Ca^{2+}-independent process is likely disrupted in these larvae. The decreased probability of release observed in polylysine motif mutants, coupled with their slow rate of recovery from depression, is consistent with the hypothesis that Ca^{2+}-independent docking/priming of synaptic vesicles is disrupted in these mutants. The fact that the polylysine mutation abolished the ability of synaptotagmin to accelerate Ca^{2+}-independent, SNARE-mediated fusion provides direct support for this hypothesis. Thus, we propose that the major role of the polylysine motif of synaptotagmin during the synaptic vesicle cycle in vivo is to facilitate Ca^{2+}-independent priming of synaptic vesicles at release sites.

ACKNOWLEDGMENTS

We thank Dr. Suzanne Royer for technical assistance with electron microscopy and Brie Paddock for assistance with PyMOL. This work was supported by National Science Foundation Grant 9982862 and National Institute of Health Grant NS-045865.

REFERENCES

Araç, D., Chen, X., Khant, H. A., Ubach, J., Ludtke, S. J., Kikkawa, M., Johnson, A. E., Chiu, W., Südhof, T. C., and Rizo, J. (2006). Close membrane-membrane proximity induced by Ca(2+)-dependent multivalent binding of synaptotagmin-1 to phospholipids. Nat. Struct. Mol. Biol. *13*, 209–217.

Aravamudan, B., Fergestad, T., Davis, W. S., Rodesch, C. K., and Broadie, K. (1999). *Drosophila* UNC-13 is essential for synaptic transmission. Nat. Neurosci. *2*, 965–971.

Atwood, H. L., and Karunanithi, S. (2002). Diversification of synaptic strength: presynaptic elements. Nat. Rev. Neurosci. *3*, 497–516.

Augustine, G. J. (2001). How does calcium trigger neurotransmitter release? Curr. Opin. Neurobiol. *11*, 320–326.

Bai, J., and Chapman, E. R. (2004). The C2 domains of synaptotagmin–partners in exocytosis. Trends Biochem. Sci. *29*, 143–151.

Bai, J., Earles, C. A., Lewis, J. L., and Chapman, E. R. (2000). Membrane-embedded synaptotagmin penetrates cis or trans target membranes and clusters via a novel mechanism. J. Biol. Chem. *275*, 25427–25435.

Bai, J., Tucker, W. C., and Chapman, E. R. (2004). PIP2 increases the speed of response of synaptotagmin and steers its membrane-penetration activity toward the plasma membrane. Nat. Struct. Mol. Biol. *11*, 36–44.

Bai, J., Wang, P., and Chapman, E. R. (2002). C2A activates a cryptic Ca(2+)-triggered membrane penetration activity within the C2B domain of synaptotagmin I. Proc. Natl. Acad. Sci. USA *99*, 1665–1670.

Betz, W. J., Mao, F., and Bewick, G. S. (1992). Activity-dependent fluorescent staining and destaining of living vertebrate motor nerve terminals. J. Neurosci. *12*, 363–375.

Bhalla, A., Chicka, M. C., Tucker, W. C., and Chapman, E. R. (2006). Ca(2+)-synaptotagmin directly regulates t-SNARE function during reconstituted membrane fusion. Nat. Struct. Mol. Biol. *13*, 323–330.

Bollmann, J. H., Sakmann, B., and Borst, J. G. (2000). Calcium sensitivity of glutamate release in a calyx-type terminal. Science *289*, 953–957.

Borden, C. R., Stevens, C. F., Sullivan, J. M., and Zhu, Y. (2005). Synaptotagmin mutants Y311N and K326/327A alter the calcium dependence of neurotransmission. Mol. Cell. Neurosci. *29*, 462–470.

Brose, N., Petrenko, A. G., Südhof, T. C., and Jahn, R. (1992). Synaptotagmin: a calcium sensor on the synaptic vesicle surface. Science *256*, 1021–1025.

Capogna, M., McKinney, R. A., O'Connor, V., Gähwiler, B. H., and Thompson, S. M. (1997). Ca2+ or Sr2+ partially rescues synaptic transmission in hippocampal cultures treated with botulinum toxin A and C, but not tetanus toxin. J. Neurosci. *17*, 7190–7202.

Chapman, E. R., Desai, R. C., Davis, A. F., and Tornehl, C. K. (1998). Delineation of the oligomerization, AP-2 binding, and synprint binding region of the C2B domain of synaptotagmin. J. Biol. Chem. *273*, 32966–32972.

Chen, B. M., and Grinnell, A. D. (1997). Kinetics, Ca2+ dependence, and biophysical properties of integrin-mediated mechanical modulation of transmitter release from frog motor nerve terminals. J. Neurosci. *17*, 904–916.

Cremona, O., and De Camilli, P. (2001). Phosphoinositides in membrane traffic at the synapse. J. Cell Sci. *114*, 1041–1052.

DeLano, W. L. (2002). The PyMOL Molecular Graphics System. http://www.pymol.org.

Delgado, R., Maureira, C., Oliva, C., Kidokoro, Y., and Labarca, P. (2000). Size of vesicle pools, rates of mobilization, and recycling at neuromuscular synapses of a *Drosophila* mutant, shibire. Neuron *28*, 941–953.

Dodge, F. A., Jr., and Rahamimoff, R. (1967). Co-operative action of calcium ions in transmitter release at the neuromuscular junction. J. Physiol. *193*, 419–432.

Fatt, P., and Katz, B. (1952). Spontaneous subthreshold activity at the motor nerve endings. J. Physiol. *117*, 109–128.

Fernandez, I., Ubach, J., Dulubova, I., Zhang, X., Südhof, T. C., and Rizo, J. (1998). Three-dimensional structure of an evolutionarily conserved N-terminal domain of syntaxin 1A. Cell *94*, 841–849.

Fernández-Chacón, R., Königstorfer, A., Gerber, S. H., García, J., Matos, M. F., Stevens, C. F., Brose, N., Rizo, J., Rosenmund, C., and Südhof, T. C. (2001). Synaptotagmin I functions as a calcium regulator of release probability. Nature *410*, 41–49.

Fernández-Chacón, R., Shin, O. H., Königstorfer, A., Matos, M. F., Meyer, A. C., Garcia, J., Gerber, S. H., Rizo, J., Südhof, T. C., and Rosenmund, C. (2002). Structure/function analysis of Ca2+ binding to the C2A domain of synaptotagmin 1. J. Neurosci. *22*, 8438–8446.

Geppert, M., Goda, Y., Hammer, R. E., Li, C., Rosahl, T. W., Stevens, C. F., and Südhof, T. C. (1994). Synaptotagmin I: a major Ca2+ sensor for transmitter release at a central synapse. Cell *79*, 717–727.

Grass, I., Thiel, S., Höning, S., and Haucke, V. (2004). Recognition of a basic AP-2 binding motif within the C2B domain of synaptotagmin is dependent on multimerization. J. Biol. Chem. *279*, 54872–54880.

Guichet, A., Wucherpfennig, T., Dudu, V., Etter, S., Wilsch-Bräuniger, M., Hellwig, A., González-Gaitán, M., Huttner, W. B., and Schmidt, A. A. (2002). Essential role of endophilin A in synaptic vesicle budding at the *Drosophila* neuromuscular junction. EMBO J. *21*, 1661–1672.

Hagiwara, S., and Takahashi, K. (1967). Surface density of calcium ions and calcium spikes in the barnacle muscle fiber membrane. J. Gen. Physiol. *50*, 583–601.

Haucke, V., and De Camilli, P. (1999). AP-2 recruitment to synaptotagmin stimulated by tyrosine-based endocytic motifs. Science *285*, 1268–1271.

Haucke, V., Wenk, M. R., Chapman, E. R., Farsad, K., and De Camilli, P. (2000). Dual interaction of synaptotagmin with mu2- and alpha-adaptin facilitates clathrin-coated pit nucleation. EMBO J. *19*, 6011–6019.

Heidelberger, R., Heinemann, C., Neher, E., and Matthews, G. (1994). Calcium dependence of the rate of exocytosis in a synaptic terminal. Nature *371*, 513–515.

Holz, R. W., Hlubek, M. D., Sorensen, S. D., Fisher, S. K., Balla, T., Ozaki, S., Prestwich, G. D., Stuenkel, E. L., and Bittner, M. A. (2000). A pleckstrin homology domain specific for phosphatidylinositol 4,5-bisphosphate (PtdIns-4,5-P2) and fused to green fluorescent protein identifies plasma membrane PtdIns-4,5-P2 as being important in exocytosis. J. Biol. Chem. *275*, 17878–17885.

Hurley, J. H., and Wendland, B. (2002). Endocytosis: driving membranes around the bend. Cell *111*, 143–146.

Jan, L. Y., and Jan, Y. N. (1976). Properties of the larval neuromuscular junction in *Drosophila melanogaster*. J. Physiol. *262*, 189–214.

Jarousse, N., and Kelly, R. B. (2001). The AP2 binding site of synaptotagmin 1 is not an internalization signal but a regulator of endocytosis. J. Cell Biol. *154*, 857–866.

Jarousse, N., Wilson, J. D., Araç, D., Rizo, J., and Kelly, R. B. (2003). Endocytosis of synaptotagmin 1 is mediated by a novel, tryptophan-containing motif. Traffic *4*, 468–478.

Jorgensen, E. M., Hartwieg, E., Schuske, K., Nonet, M. L., Jin, Y., and Horvitz, H. R. (1995). Defective recycling of synaptic vesicles in synaptotagmin mutants of *Caenorhabditis elegans*. Nature *378*, 196–199.

Karunanithi, S., Georgiou, J., Charlton, M. P., and Atwood, H. L. (1997). Imaging of calcium in *Drosophila* larval motor nerve terminals. J. Neurophysiol. *78*, 3465–3467.

Kashani, A. H., Chen, B. M., and Grinnell, A. D. (2001). Hypertonic enhancement of transmitter release from frog motor nerve terminals: Ca2+ independence and role of integrins. J. Physiol. *530*, 243–252.

Kim, W. T., Chang, S., Daniell, L., Cremona, O., Di Paolo, G., and De Camilli, P. (2002). Delayed reentry of recycling vesicles into the fusion-competent synaptic vesicle pool in synaptojanin 1 knockout mice. Proc. Natl. Acad. Sci. USA *99*, 17143–17148.

Koenig, J. H., Kosaka, T., and Ikeda, K. (1989). The relationship between the number of synaptic vesicles and the amount of transmitter released. J. Neurosci. *9*, 1937–1942.

Kuromi, H., and Kidokoro, Y. (1998). Two distinct pools of synaptic vesicles in single presynaptic boutons in a temperature-sensitive *Drosophila* mutant, shibire. Neuron *20*, 917–925.

Li, L., Shin, O. H., Rhee, J. S., Araç, D., Rah, J. C., Rizo, J., Südhof, T., and Rosenmund, C. (2006). Phosphatidylinositol phosphates as co-activators of Ca2+ binding to C2 domains of synaptotagmin 1. J. Biol. Chem. *281*, 15845–15852.

Littleton, J. T., Bai, J., Vyas, B., Desai, R., Baltus, A. E., Garment, M. B., Carlson, S. D., Ganetzky, B., and Chapman, E. R. (2001). *synaptotagmin* mutants reveal essential functions for the C2B domain in Ca2+-triggered fusion and recycling of synaptic vesicles *in vivo*. J. Neurosci. *21*, 1421–1433.

Littleton, J. T., Stern, M., Perin, M., and Bellen, H. J. (1994). Calcium dependence of neurotransmitter release and rate of spontaneous vesicle fusions are altered in *Drosophila* synaptotagmin mutants. Proc. Natl. Acad. Sci. USA *91*, 10888–10892.

Llinás, R. R., Sugimori, M., Moran, K. A., Moreira, J. E., and Fukuda, M. (2004). Vesicular reuptake inhibition by a synaptotagmin I C2B domain antibody at the squid giant synapse. Proc. Natl. Acad. Sci. USA *101*, 17855–17860.

Loewen, C. A., Royer, S. M., and Reist, N. E. (2006). *Drosophila* synaptotagmin I null mutants show severe alterations in vesicle populations but calcium-binding motif mutants do not. J. Comp. Neurol. *496*, 1–12.

Lu, X., Xu, Y., Zhang, F., and Shin, Y. K. (2006). Synaptotagmin I and Ca(2+) promote half fusion more than full fusion in SNARE-mediated bilayer fusion. FEBS letters *580*, 2238–2246.

Lu, X., Zhang, F., McNew, J. A., and Shin, Y. K. (2005). Membrane fusion induced by neuronal SNAREs transits through hemifusion. J. Biol. Chem. *280*, 30538–30541.

Mackler, J. M., Drummond, J. A., Loewen, C. A., Robinson, I. M., and Reist, N. E. (2002). The C2B Ca2+-binding motif of synaptotagmin is required for synaptic transmission *in vivo*. Nature *418*, 340–344.

Mackler, J. M., and Reist, N. E. (2001). Mutations in the second C2 domain of synaptotagmin disrupt synaptic transmission at *Drosophila* neuromuscular junctions. J. Comp. Neurol. *436*, 4–16.

Macleod, G. T., Hegström-Wojtowicz, M., Charlton, M. P., and Atwood, H. L. (2002). Fast calcium signals in *Drosophila* motor neuron terminals. J. Neurophysiol. *88*, 2659–2663.

Mahal, L. K., Sequeira, S. M., Gureasko, J. M., and Söllner, T. H. (2002). Calcium-independent stimulation of membrane fusion and SNAREpin formation by synaptotagmin I. J. Cell Biol. *158*, 273–282.

Marrus, S. B., Portman, S. L., Allen, M. J., Moffat, K. G., and DiAntonio, A. (2004). Differential localization of glutamate receptor subunits at the *Drosophila* neuromuscular junction. J. Neurosci. *24*, 1406–1415.

Martin, A. R. (1955). A further study of the statistical composition of the endplate potential. J. Physiol. *130*, 114–122.

Martin, T. F. (2003). Tuning exocytosis for speed: fast and slow modes. Biochim. Biophys. Acta *1641*, 157–165.

McLachlan, E. M., and Martin, A. R. (1981). Non-linear summation of endplate potentials in the frog and mouse. J. Physiol. *311*, 307–324.

Micheva, K. D., Holz, R. W., and Smith, S. J. (2001). Regulation of presynaptic phosphatidylinositol 4,5-biphosphate by neuronal activity. J. Cell Biol. *154*, 355–368.

Mochida, S., Yokoyama, C. T., Kim, D. K., Itoh, K., and Catterall, W. A. (1998). Evidence for a voltage-dependent enhancement of neurotransmitter release mediated via the synaptic protein interaction site of N-type Ca2+ channels. Proc. Natl. Acad. Sci. USA *95*, 14523–14528.

Nicholson-Tomishima, K., and Ryan, T. A. (2004). Kinetic efficiency of endocytosis at mammalian CNS synapses requires synaptotagmin I. Proc. Natl. Acad. Sci. USA *101*, 16648–16652.

Nishiki, T., and Augustine, G. J. (2004). Dual roles of the C2B domain of synaptotagmin I in synchronizing Ca2+-dependent neurotransmitter release. J. Neurosci. *24*, 8542–8550.

Okamoto, T., Tamura, T., Suzuki, K., and Kidokoro, Y. (2005). External Ca2+ dependency of synaptic transmission in *Drosophila* synaptotagmin I mutants. J. Neurophysiol. *94*, 1574–1586.

Parlati, F., Weber, T., McNew, J. A., Westermann, B., Söllner, T. H., and Rothman, J. E. (1999). Rapid and efficient fusion of phospholipid vesicles by the alpha-helical core of a SNARE complex in the absence of an N-terminal regulatory domain. Proc. Natl. Acad. Sci. USA *96*, 12565–12570.

Perin, M. S., Brose, N., Jahn, R., and Südhof, T. C. (1991). Domain structure of synaptotagmin (p65). J. Biol. Chem. *266*, 623–629.

Poskanzer, K. E., Fetter, R. D., and Davis, G. W. (2006). Discrete residues in the c(2)b domain of synaptotagmin I independently specify endocytic rate and synaptic vesicle size. Neuron *50*, 49–62.

Poskanzer, K. E., Marek, K. W., Sweeney, S. T., and Davis, G. W. (2003). Synaptotagmin I is necessary for compensatory synaptic vesicle endocytosis *in vivo*. Nature *426*, 559–563.

Pyle, J. L., Kavalali, E. T., Piedras-Rentería, E. S., and Tsien, R. W. (2000). Rapid reuse of readily releasable pool vesicles at hippocampal synapses. Neuron *28*, 221–231.

Qin, G., Schwarz, T., Kittel, R. J., Schmid, A., Rasse, T. M., Kappei, D., Ponimaskin, E., Heckmann, M., and Sigrist, S. J. (2005). Four different subunits are essential for expressing the synaptic glutamate receptor at neuromuscular junctions of *Drosophila*. J. Neurosci. *25*, 3209–3218.

Reist, N. E., Buchanan, J., Li, J., DiAntonio, A., Buxton, E. M., and Schwarz, T. L. (1998). Morphologically docked synaptic vesicles are reduced in synaptotagmin mutants of *Drosophila*. J. Neurosci. *18*, 7662–7673.

Rhee, J. S., Li, L. Y., Shin, O. H., Rah, J. C., Rizo, J., Südhof, T. C., and Rosenmund, C. (2005). Augmenting neurotransmitter release by enhancing the apparent Ca2+ affinity of synaptotagmin 1. Proc. Natl. Acad. Sci. USA *102*, 18664–18669.

Richards, D. A., Guatimosim, C., Rizzoli, S. O., and Betz, W. J. (2003). Synaptic vesicle pools at the frog neuromuscular junction. Neuron *39*, 529–541.

Rickman, C., Archer, D. A., Meunier, F. A., Craxton, M., Fukuda, M., Burgoyne, R. D., and Davletov, B. (2004). Synaptotagmin interaction with the syntaxin/SNAP-25 dimer is mediated by an evolutionarily conserved motif and is sensitive to inositol hexakisphosphate. J. Biol. Chem. *279*, 12574–12579.

Rickman, C., Jiménez, J. L., Graham, M. E., Archer, D. A., Soloviev, M., Burgoyne, R. D., and Davletov, B. (2006). Conserved prefusion protein assembly in regulated exocytosis. Mol. Biol. Cell *17*, 283–294.

Rosenmund, C., and Stevens, C. F. (1996). Definition of the readily releasable pool of vesicles at hippocampal synapses. Neuron *16*, 1197–1207.

Ryan, T. A., Li, L., Chin, L. S., Greengard, P., and Smith, S. J. (1996). Synaptic vesicle recycling in synapsin I knock-out mice. J. Cell Biol. *134*, 1219–1227.

Sankaranarayanan, S., and Ryan, T. A. (2001). Calcium accelerates endocytosis of vSNAREs at hippocampal synapses. Nat. Neurosci. *4*, 129–136.

Schikorski, T., and Stevens, C. F. (2001). Morphological correlates of functionally defined synaptic vesicle populations. Nat. Neurosci. *4*, 391–395.

Stevens, C. F., and Tsujimoto, T. (1995). Estimates for the pool size of releasable quanta at a single central synapse and for the time required to refill the pool. Proc. Natl. Acad. Sci. USA *92*, 846–849.

Stewart, B. A., Atwood, H. L., Renger, J. J., Wang, J., and Wu, C. F. (1994). Improved stability of *Drosophila* larval neuromuscular preparations in haemolymph-like physiological solutions. J. Comp. Physiol. A *175*, 179–191.

Stewart, B. A., Mohtashami, M., Trimble, W. S., and Boulianne, G. L. (2000). SNARE proteins contribute to calcium cooperativity of synaptic transmission. Proc. Natl. Acad. Sci. USA *97*, 13955–13960.

Stimson, D. T., Estes, P. S., Rao, S., Krishnan, K. S., Kelly, L. E., and Ramaswami, M. (2001). *Drosophila* stoned proteins regulate the rate and fidelity of synaptic vesicle internalization. J. Neurosci. *21*, 3034–3044.

Suzuki, K., Grinnell, A. D., and Kidokoro, Y. (2002a). Hypertonicity-induced transmitter release at *Drosophila* neuromuscular junctions is partly mediated by integrins and cAMP/protein kinase A. J. Physiol. *538*, 103–119.

Suzuki, K., Okamoto, T., and Kidokoro, Y. (2002b). Biphasic modulation of synaptic transmission by hypertonicity at the embryonic *Drosophila* neuromuscular junction. J. Physiol. *545*, 119–131.

Suzuki, S., Osanai, M., Murase, M., Suzuki, N., Ito, K., Shirasaki, T., Narita, K., Ohnuma, K., Kuba, K., and Kijima, H. (2000). Ca2+ dynamics at the frog motor nerve terminal. Pflueg. Arch. Eur. J. Physiol. *440*, 351–365.

Takei, K., and Haucke, V. (2001). Clathrin-mediated endocytosis: membrane factors pull the trigger. Trends Cell Biol. *11*, 385–391.

Verstreken, P., Kjaerulff, O., Lloyd, T. E., Atkinson, R., Zhou, Y., Meinertzhagen, I. A., and Bellen, H. J. (2002). Endophilin mutations block clathrin-mediated endocytosis but not neurotransmitter release. Cell *109*, 101–112.

Verstreken, P., Koh, T. W., Schulze, K. L., Zhai, R. G., Hiesinger, P. R., Zhou, Y., Mehta, S. Q., Cao, Y., Roos, J., and Bellen, H. J. (2003). Synaptojanin is recruited by endophilin to promote synaptic vesicle uncoating. Neuron *40*, 733–748.

von Poser, C., Zhang, J. Z., Mineo, C., Ding, W., Ying, Y., Südhof, T. C., and Anderson, R. G. (2000). Synaptotagmin regulation of coated pit assembly. J. Biol. Chem. *275*, 30916–30924.

Wang, C. T., Grishanin, R., Earles, C. A., Chang, P. Y., Martin, T. F., Chapman, E. R., and Jackson, M. B. (2001). Synaptotagmin modulation of fusion pore kinetics in regulated exocytosis of dense-core vesicles. Science *294*, 1111–1115.

Wang, P., Wang, C. T., Bai, J., Jackson, M. B., and Chapman, E. R. (2003). Mutations in the effector binding loops in the C2A and C2B domains of synaptotagmin I disrupt exocytosis in a nonadditive manner. J. Biol. Chem. *278*, 47030–47037.

Weber, T., Parlati, F., McNew, J. A., Johnston, R. J., Westermann, B., Sèollner, T. H., and Rothman, J. E. (2000). SNAREpins are functionally resistant to disruption by NSF and alphaSNAP. J. Cell Biol. *149*, 1063–1072.

Weber, T., Zemelman, B. V., McNew, J. A., Westermann, B., Gmachl, M., Parlati, F., Sèollner, T. H., and Rothman, J. E. (1998). SNAREpins: minimal machinery for membrane fusion. Cell *92*, 759–772.

Wu, L. G., and Betz, W. J. (1996). Nerve activity but not intracellular calcium determines the time course of endocytosis at the frog neuromuscular junction. Neuron *17*, 769–779.

Wu, Y., He, Y., Bai, J., Ji, S. R., Tucker, W. C., Chapman, E. R., and Sui, S. F. (2003). Visualization of synaptotagmin I oligomers assembled onto lipid monolayers. Proc. Natl. Acad. Sci. USA *100*, 2082–2087.

Wucherpfennig, T., Wilsch-Bräuninger, M., and González-Gaitán, M. (2003). Role of *Drosophila* Rab5 during endosomal trafficking at the synapse and evoked neurotransmitter release. J. Cell Biol. *161*, 609–624.

Xu, T., Rammner, B., Margittai, M., Artalejo, A. R., Neher, E., and Jahn, R. (1999). Inhibition of SNARE complex assembly differentially affects kinetic components of exocytosis. Cell *99*, 713–722.

Xu, Y., Zhang, F., Su, Z., McNew, J. A., and Shin, Y. K. (2005). Hemifusion in SNARE-mediated membrane fusion. Nat. Struct. Mol. Biol. *12*, 417–422.

Yoshihara, M., and Littleton, J. T. (2002). Synaptotagmin I functions as a calcium sensor to synchronize neurotransmitter release. Neuron *36*, 897–908.

Zhang, J. Z., Davletov, B. A., Südhof, T. C., and Anderson, R. G. (1994). Synaptotagmin I is a high affinity receptor for clathrin AP-2, implications for membrane recycling. Cell *78*, 751–760.

Zucker, R. S., and Regehr, W. G. (2002). Short-term synaptic plasticity. Annu. Rev. Physiol. *64*, 355–405.